Title

A novel inhibitor of p75-neurotrophin receptor improves functional outcomes in two models of traumatic brain injury.

Journal

Brain : a journal of neurology, 139(Pt 6)

ISSN

0006-8950

Authors

Delbary-Gossart, Sandrine
Lee, Sangmi
Baroni, Marco
et al.

Publication Date

2016-06-01

DOI

10.1093/brain/aww074

Peer reviewed

doi:10.1093/brain/aww074 BRAIN 2016: 139; 1762–1782 | 1762

BRAIN
A JOURNAL OF NEUROLOGY

A novel inhibitor of p75-neurotrophin receptor improves functional outcomes in two models of traumatic brain injury

Sandrine Delbary-Gossart,[1,*] Sangmi Lee,[2,*] Marco Baroni,[3] Isabelle Lamarche,[4] Michele Arnone,[4] Benoit Canolle,[4] Amity Lin,[2] Jeffrey Sacramento,[2] Ernesto A. Salegio,[2] Marie-Noelle Castel,[4] Nathalie Delesque-Touchard,[4] Antoine Alam,[4] Patricia Laboudie,[4] Badia Ferzaz,[4] Pierre Savi,[4] Jean-Marc Herbert,[4] Geoffrey T. Manley,[2] Adam R. Ferguson,[2] Jacqueline C. Bresnahan,[2] Françoise Bono[1] and Michael S. Beattie[2]

[*]These authors contributed equally to this work.

The p75 neurotrophin receptor is important in multiple physiological actions including neuronal survival and neurite outgrowth during development, and after central nervous system injury. We have discovered a novel piperazine-derived compound, EVT901, which interferes with p75 neurotrophin receptor oligomerization through direct interaction with the first cysteine-rich domain of the extracellular region. Using ligand binding assays with cysteine-rich domains-fused p75 neurotrophin receptor, we confirmed that EVT901 interferes with oligomerization of full-length p75 neurotrophin receptor in a dose-dependent manner. Here we report that EVT901 reduces binding of pro-nerve growth factor to p75 neurotrophin receptor, blocks pro-nerve growth factor induced apoptosis in cells expressing p75 neurotrophin receptor, and enhances neurite outgrowth *in vitro*. Furthermore, we demonstrate that EVT901 abrogates p75 neurotrophin receptor signalling by other ligands, such as prion peptide and amyloid-β. To test the efficacy of EVT901 *in vivo*, we evaluated the outcome in two models of traumatic brain injury. We generated controlled cortical impacts in adult rats. Using unbiased stereological analysis, we found that EVT901 delivered intravenously daily for 1 week after injury, reduced lesion size, protected cortical neurons and oligodendrocytes, and had a positive effect on neurological function. After lateral fluid percussion injury in adult rats, oral treatment with EVT901 reduced neuronal death in the hippocampus and thalamus, reduced long-term cognitive deficits, and reduced the occurrence of post-traumatic seizure activity. Together, these studies provide a new reagent for altering p75 neurotrophin receptor actions after injury and suggest that EVT901 may be useful in treatment of central nervous system trauma and other neurological disorders where p75 neurotrophin receptor signalling is affected.

1 Evotec, 195 route d'Espagne, 31036 Toulouse cedex, France
2 Brain and Spinal Injury Center, Department of Neurological Surgery, University of California, San Francisco, 1001 Potrero Ave, San Francisco, CA 94110, USA
3 Sanofi Research, Exploratory Unit, Via Gaetano Sbodio 2, 20134 Milano, Italy
4 From Sanofi Research, Early to Candidate, 195 route d'Espagne, 31036 Toulouse cedex, France

Correspondence to: Michael S. Beattie, PhD,
Brain and Spinal Injury Center, Department of Neurological Surgery,
Box 0899, University of California at San Francisco,
1001 Potrero Ave, Bldg 1, Rm 101, San Francisco, CA 94143, USA
E-mail: Michael.Beattie@ucsf.edu

Received October 28, 2015. Revised February 05, 2016. Accepted February 20, 2016. Advance Access publication April 15, 2016

Correspondence may also be addressed to: Françoise Bono, Evotec, 195 route d'Espagne, 31036 Toulouse, France
E-mail: Francoise.Bono@evotec.com

Keywords: p75NTR; TBI; EVT901; neuron; oligodendrocyte

Abbreviations: CCI = controlled cortical impact; CRD = cysteine rich domain; FPI = fluid percussion injury; OPC = oligodendrocyte precursor cell; PLAD = pre-ligand-binding assembling domain; p75NTR = p75 neurotrophin receptor; TBI = traumatic brain injury; TNFR = TNF receptor; Trk = tropomyosin receptor kinase

Introduction

The p75 neurotrophin receptor (p75NTR, encoded by *NGFR*) is a transmembrane glycoprotein member of the TNF receptor (TNFR) superfamily, characterized by four cysteine-rich domains (CRDs) in its extracellular region (Underwood and Coulson, 2008). P75NTR binds to all neurotrophins with similar affinity (10^{-9} M) to mediate various functions (Hempstead, 2002). p75NTR as a monomer can interact with tropomyosin receptor kinase (Trk; TrkA, B and C, encoded by *NTRK1*, *NTRK2* and *NTRK3*, respectively) and potentiate Trk signalling, leading to neuronal survival, neurite outgrowth, and axonal regeneration (Chan *et al.*, 2000). However, p75NTR can also mediate cell death through pro-apoptotic signalling in neurons, oligodendrocytes and Schwann cells, linked to the binding of pro-neurotrophins (pro-NGF, pro-BDNF) (Chan *et al.*, 2000; Beattie *et al.*, 2002; Roux and Barker, 2002; Gentry *et al.*, 2004; Underwood and Coulson, 2008). Recent work has also shown that aggregated oligomers (prion peptide fragment PrP, amyloid peptide) interact with p75NTR leading to cell death *in vitro* (Dechant and Barde, 2002; Hempstead, 2002; Roux and Barker, 2002; Gentry *et al.*, 2004), and that p75NTR oligomers cooperate with many different protein partners (Nogo receptor, LINGO1, sortilin) to form multimeric receptor complexes leading to apoptosis and axonal outgrowth inhibition (Nykjaer *et al.*, 2005; Hempstead, 2006).

Many TNFR superfamily members exist as pre-assembled oligomers on the cell surface before ligand binding, through a specific self-association domain, the pre-ligand assembly domain (PLAD; Chan *et al.*, 2000). This amino acid sequence, located in the CRD1 of the receptor, mediates receptor assembly, allowing ligand binding and receptor functioning (Chan, 2007). Such a domain has not yet been identified for p75NTR.

Although p75NTR is mainly expressed as a 75 kDa transmembrane glycoprotein, there is a protein isoform of p75NTR (s-p75NTR) that arises from alternative splicing of exon III and lacks the CRDs 2–4 (Roux and Barker, 2002). Soluble p75NTR (s-p75NTR) is critical for development of both the nervous and vascular systems (von Schack *et al.*, 2001). Although s-p75NTR is unable to bind neurotrophins, cross-linked s-p75NTR might be activated through the pre-ligand assembly domain (Della-Bianca *et al.*, 2001; Yaar *et al.*, 2002).

P75NTR expression is limited in adulthood to some peripheral tissues and a few brain regions (Schor, 2005). However, injury-induced p75NTR expression has been reported *in vivo* in various CNS pathologies (Beattie *et al.*, 2002; Dechant and Barde, 2002; Turner *et al.*, 2004; Diarra *et al.*, 2009). Reduction of p75NTR activity can protect cortical neurons from cell death after close axotomy (Harrington *et al.*, 2004), and a novel peptide antagonist of the p75NTR protects oligodendrocytes after spinal cord injury and promotes better neurological recovery (Tep *et al.*, 2013). Thus, p75NTR interactions with co-receptors could provide a target for both neuroprotection and enhancement of axonal growth, if it were possible to reduce p75NTR homodimerization or interactions with 'negative' co-receptors while simultaneously enhancing heterodimerization with TrkA. To that end, we attempted to find selective inhibitors of p75NTR pre-ligand dimerization able to block both s-p75NTR and p75NTR signalling, and to modulate Trks/p75NTR signalling. Recently, we identified EVT901 as such an antagonist of p75NTR, and here, report that EVT901 inhibits p75NTR oligomerization *in vitro* while increasing TrkA phosphorylation, blocks apoptosis and increases neurite outgrowth in neuroblastoma cells. In cortical oligodendrocyte cultures, EVT901 reduced p75NTR expression and cell death produced by proNGF. *In vivo*, traumatic brain injury (TBI) increased the expression of both p75NTR and proNGF in both controlled cortical impact (CCI-TBI) and fluid percussion injury (FPI-TBI) models of TBI, and EVT901 showed neuroprotection in both models, and reduced post-TBI seizure susceptibility. Together, these results suggest the utility of targeting p75NTR oligomerization in CNS trauma, and provide a novel drug that may be useful in CNS injuries and neurodegenerative disorders.

Materials and methods

Animals

Adult male Long-Evans rats (~225 g, Simonsen Laboratories) were used for CCI-TBI study. All animal experiments were approved by the Institutional Laboratory Animal Care and Use Committee of University of California San Francisco and performed in compliance with NIH guidelines. Adult male Sprague Dawley rats (170–230 g, strain RjHan) were used for the FPI-TBI study. All animal treatment procedures described in this aspect of the study were approved by the Animal Care and Use Committee of Sanofi. The animal facilities are fully accredited by Association for Assessment and Accreditation of Laboratory Animal Care International

(AAALAC). Rats were housed individually and maintained on a 12 h light/dark cycle with free access to food and water.

In vitro assays to examine EVT901 effects on p75NTR oligomerization

Human cell lines

Human Embryonic Kidney (HEK) 293T cells and human neuroblastoma SHSY-5Y cells were from ATCC [authenticated by the provider using short tandem repeat (STR) profiling]. Neuroblastoma SK-N-BE p75NTR (BEp75) cell line, stably expressing the human full-length p75NTR, was kindly provided by Della Valle G (Department of Genetics and Microbiology, University of Pavia, Italy), and the molecular analyses have been previously described (Bunone *et al.*, 1997). All cell lines were maintained in appropriate media supplemented with foetal calf serum and glutamine and were tested for mycoplasma contamination.

Construction of p75NTR-tagged proteins

The human full-length p75NTR was reverse-transcribed and amplified from SKNBE-p75NTR cells. The PCR product was subcloned into the pDisplay vector to obtain the construct HA-p75NTR or into pCMV-Tag4A to obtain Flag-p75NTR. The CRD1p75NTR construct, inserted into the pDisplay vector, contains sequences representing the first CRD (AA29-64) directly linked to amino acid residues 214–427 of the receptor p75NTR (deletion of CRD2–4). Chimera CRD1-CD40 is composed of the first CRD of p75NTR (AA29-64, fragment 1) linked to human CD40 receptor deleted in CRD1 (AA60-277, fragment 2) inserted into the pDisplay vector. The human CD40 full-length (AA1-277) was cloned into the pCI-neo vector (Fig. 1E).

Concerning the AP-p75NTR construct, alkaline phosphatase (AP) was fused to the NH_2-terminus of the extracellular domain of the receptor p75NTR (containing the CRDs 1–4) and cloned into pcDNA-FRTV5His TOPO® vector to obtain a soluble form of p75NTR tagged with alkaline phosphatase. All the resulting cDNAs for the different constructs were sequenced to verify the correct reading frame.

Binding of soluble AP-p75NTR

Binding experiments were performed on SKNBE-p75NTR using a soluble form of the receptor p75NTR fused to alkaline phosphatase (AP-p75NTR) as ligand obtained after transient transfection of HEK293T cells for 3 days. Briefly, SKNBE-p75NTR cells (2.5×10^4 cells/well) were plated in 96-well plates for 24 h, and preincubated (37 °C) for 1 h with increasing concentrations of EVT901 followed by addition of 10 nM AP-p75NTR for 1 h. Cells were filtered (Skatron), separately collected with addition of specific substrate (CDP star) for measurement of alkaline phosphatase activity.

Binding of NGF

Binding of ^{125}I-NGF (2000 Ci/mM, Amersham) was carried out on cell suspensions of SK-N-BE cells according to the method described by Weskamp and Reichardt (1991). The specific binding was defined as the difference between the total binding and the non-specific binding [measured after 1 h of preincubation of the cells with unlabelled NGF (1 μM)]. Competition experiments were done with 0.3 nM of ^{125}I-NGF and preincubation with increasing doses of EVT901.

Oligomerization of tagged p75NTR

HEK293T cells (3×10^6 cells/flask) were transiently co-transfected for 24 h with equal amount of DNA from the p75NTR full-length tagged either in NH_2-terminal with an haemagglutinin A epitope tag (HA) (HA-p75NTR) or in C-terminal with a Flag epitope tag (Flag-p75NTR), using the FuGENE® 6 reagent (Roche Applied System). After treatment for 24 h with EVT901, cells were lysed and the supernatants were collected. Equal amounts of proteins were dispatched onto anti-flag M2 coated 96 well plates (Sigma-Aldrich) for 1 h at room temperature, followed by washing, incubation with anti-HA horseradish peroxidase (HRP), and reaction with specific substrate. Quantification was measured using a microplate fluorometer and expressed as OD (450 nm reading). Error bar indicates ± standard error of the mean (SEM).

Induction of cell death

SH-SY5Y cells (1.5×10^6 cells/ml in 35-mm collagen-coated dishes) were stimulated for 48 h with pro-NGF (10 ng/ml, SCIL proteins), $PrP_{106-126}$ (25 μM, Bachem), or amyloid-β_{1-40} (10 μM, Bachem) in presence or not of EVT901. Apoptosis was evaluated with a photometric enzyme immunoassay (cell death detection ELISA, Roche) for the quantitative detection of cytoplasmic mono- and oligonucleosomes. Results are expressed as per cent of inhibition of apoptosis versus untreated. For studies with HEK293T, cells were transiently transfected with the same amount of DNA from different constructs: empty vector (control), full-length of p75NTR (p75NTR), short-form of p75NTR (CRD1-p75NTR), full-length of CD40, or a chimera CD40-CRD1p75NTR, and for specificity studies with FAS, TNFRI, TNFRII, HVEM, LTβR, 4.1BB, or BCMA receptors. Then, cells were treated with EVT901 (100 nM) for 24 h, and apoptosis was measured and expressed as mean number of oligonucleosomes/10^6 cells. Error bar indicates ± SEM.

Neuritogenesis of SH-SY5Y cells

SH-SY5Y cells (7.5×10^4 cells/well) were incubated in collagen-coated 8-well plates overnight at 37 °C, then treated in serum-free medium, with either recombinant human NGF (10 ng/ml, R&D systems) or different concentrations of EVT901, and maintained in the same media for 3 days at 37 °C. The neurite length were visualized after staining with May-Grunwald-Giemsa and digitally photographed from randomly selected image fields.

Quantification of TrkA phosphorylation

Confluent SH-SY5Y cells were serum-deprived, and treated with NGF (10 ng/ml) or EVT901 (100 nM) for 1 to 3 days. After cell lysis, equal amounts of total protein were used for quantification of the levels of total TrkA or phosphorylated TrkA (Tyr490) using specific sandwich ELISA kits (PathScan, Cell Signaling). Results are expressed as OD_{450}. Error bar indicates ± SEM.

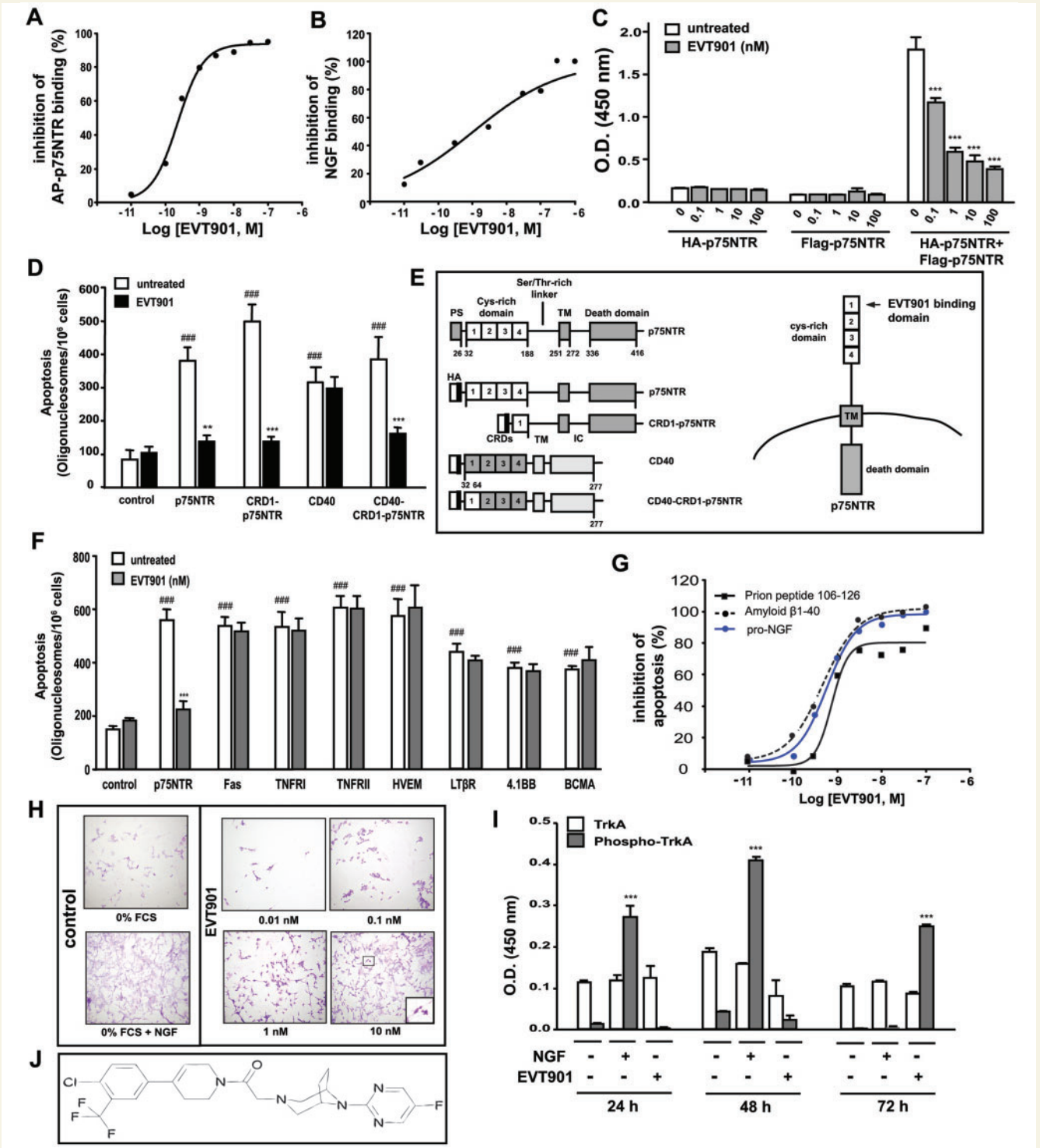

Figure 1 Mechanism of action through the CRD1 domain of p75NTR: cellular response and induction of neuritogenesis. (**A**) EVT901 inhibits the binding of AP-p75NTR to the receptor p75NTR. Binding experiments on SKN-BE-p75NTR with soluble AP-p75NTR (10 nM) in the presence of increasing concentrations of EVT901. Data are reported as mean % inhibition of binding, representative of three independent experiments. (**B**) Competition of ^{125}I-NGF binding with EVT901. Binding of ^{125}I-NGF (0.3 nM) to SKNBE-p75NTR in the presence of increasing concentrations of EVT901. Results are mean % inhibition of specific binding, representative of three independent experiments. (**C**) HEK293T cells transiently co-transfected with the same amount of DNA originating from the p75NTR full-length tagged either in C-terminal with HA (HA- p75NTR) or in N-terminal with Flag (Flag-p75NTR) and then treated or not with the compound EVT901 at 100 nM for 24 h. Oligomerization evaluated using an ELISA assay with flag-coated plates and anti-HA-HRP antibody [two-way ANOVA, EVT901 dose effect, $F(4,94) = 46.85$, $P < 0.0001$; Tag, $F(3,94) = 394.40$, $P < 0.0001$; EVT901 dose × Tag, $F(12,94) = 46.82$, $P < 0.0001$]. $^{***}P < 0.0001$ compared to 0. Data are indicated as mean ± SEM from six independent experiments. (**D** and **E**) HEK293T cells transiently transfected for 2 days with the same amount of DNA originating from the indicated constructs: empty vector (control), full-length of p75NTR (p75NTR), short-form of p75NTR (CRD1-p75NTR), full-length of CD40 (CD40),

(continued)

Primary oligodendrocyte cell culture

Primary oligodendrocyte cell culture was performed as described previously (Miller *et al.*, 2007; Veiga *et al.*, 2011). Briefly, postnatal Day 1–2 Sprague Dawley rat pups were sacrificed by decapitation and the cerebral cortices were removed and placed in the dissecting media with antibiotic/antimitotic (Sigma) containing 7.1 mg/ml $NaCl_2$, 0.36 mg/ml KCl, 0.166 mg/ml KH_2PO_4, 2.57 mg/ml D-Glucose, 2.4 mg/ml $NaHCO_3$, 0.01 mg/ml phenol red, 0.9 mg/ml bovine serum albumin (BSA) Fraction V, and 0.33 mg/ml $MgSO_4$. The cortices were minced by pipetting with a 10 ml pipette plus trypsin (10 × trypsin solution, Sigma) and incubated for 20 min at 37 °C. Next, DNase (10 × DNase, Sigma) and trypsin inhibitor (10 × trypsin inhibitor, Sigma) were added and pipetted with a 10 ml pipette until the suspension was homogenous. The suspension was filtered through 180 µm nylon net filters (Millipore) and then centrifuged at 2000 rpm for 5 min. Cells were resuspended in media [Dulbecco's modified Eagle medium (Gibco) including 10% foetal bovine serum, 292 µg/ml L-glutamine (Sigma), 1 mM sodium pyruvate (Invitrogen) and 0.04 mg/ml gentamicin (Invitrogen)], filtered through a cell strainer (40 µm nylon mesh, Fisher), and then centrifuged at 300 relative centrifugal force (rcf) for 5 min. Cells were resuspended in media. Cells were counted using a haemocytometer and placed in T-75 flasks (1.5×10^7 cells/flask). Flasks were kept in an incubator at 37 °C/5% CO_2. Media was replaced after 24 h and every 3 days thereafter. Cells were allowed to proliferate until confluent, corresponding to Day 10–14 post plating cells. Cells were shaken on an orbital shaker at 200 rpm overnight. The floating cells were collected in the 50 ml of falcon tube [split into two tubes for each oligodendrocyte precursor cell (OPC) and oligodendrocyte cells] and centrifuged at 300 rcf for 5 min. Cells were resuspended with 5 ml of either OPC media including PDGF and bFGF or oligodendrocyte media including L-thyronine and L-thyroxine. The resuspended cells were placed on 2.5 mm petri dish and incubated for 45 min. Petri dishes were then gently rinsed with media and filtered through the cell strainer (40 µm Nylon Mesh, Fisher). Cells were incubated with anti-mouse IgG magnetic beads (Invitrogen) precoated with anti-CD11b Ab (Serotec) for 30 min at 4 °C on a rocker. After washing beads with washing buffer [0.1% BSA, 2 mM EDTA, pH 7.4 in phosphate-buffered saline (PBS)], tubes were placed in a magnet holster for 2 min. The supernatant was transferred into 50 ml falcon tube. Cells were counted using a haemocytometer. Cells (2.5×10^5) were seeded into 48-well plates with poly-D-lysine coated cover glass (BD Bioscience). No serum was used during OPC/oligodendrocyte isolation to prevent OPC differentiation to oligodendrocyte cells. Each OPC and oligodendrocyte medium was replaced every day to maintain OPCs and proliferate oligodendrocyte cells, respectively, for 3 days. On Day 3, cells were treated with proNGF or/and EVT901.

Treatment with proNGF and EVT901

Studies were done to determine the optimal concentration of proNGF to induce apoptotic cell death in OPC and oligodendrocyte cultures: 0.5–100 ng/ml of proNGF (cleavage resistant mutant mouse proNGF, Alamone) was added to the OPC or oligodendrocyte media and incubated for 24 h. For reported experiments, the negative control did not contain proNGF, while the positive control contained 10 ng/ml of mature NGF (mNGF) (Harlan), and this was added to the cells and incubated for 24 h. For inhibition studies, 0, 1, 10, 30, 100, and 300 nM of EVT901 were added into the media. Mouse proNGF (50 ng/ml) was added to induce apoptotic cell death in OPC/oligodendrocyte cells and cells were kept for 24 h at 37 °C in a 5% CO_2 incubator. Sample size was determined based on previous studies (Miller *et al.*, 2007; Veiga *et al.*, 2011).

Figure 1 Continued

or a chimera of CD40 and the CRD1 domain of p75NTR (CD40-CRD1-p75NTR) (**E**), and then treated or not with the compound EVT901 at 100 nM for 24 h. Apoptosis quantified using an ELISA kit and data are expressed as mean number of oligonucleosomes/10^6 cells ± SEM, three independent experiments. Two-way ANOVA [EVT901 dose effect, $F(1,68) = 53.2$, $P < 0.0001$; constructs, $F(4,68) = 20.77$, $P < 0.0001$; EVT901 effect × constructs, $F(4,68) = 12.32$, $P < 0.0001$]. $^{**}P < 0.005$, $^{***}P < 0.001$ (EVT901 versus untreated), $^{\#\#\#}P < 0.001$ (untreated control versus untreated constructs). (**F**) HEK293T cells transiently transfected for 24 h with the indicated constructs: empty vector (control), full-length of p75NTR (p75NTR), FAS, TNFRI, TNFRII, HVEM, LTβR, 4.1BB, or BCMA receptors, and then treated or not with the compound EVT901 at 100 nM for 24 h. Apoptosis was measured and expressed as mean number of oligonucleosomes/10^6 cells ± SEM. Data are representative of two independent experiments. Two-way ANOVA [EVT901 dose effect, $F(3,134) = 8.75$, $P < 0.0001$; constructs, $F(8,134) = 28.34$, $P < 0.0001$; EVT901 dose effects × constructs, $F(6,134) = 6.75$, $P < 0.0001$]. $^{***}P < 0.001$ (EVT901 versus untreated; $^{\#\#\#}P < 0.001$ (untreated control versus untreated constructs). (**G**) Inhibition of specific p75NTR ligand-induced apoptosis. Subconfluent monolayers of SH-SY5Y cells stimulated for 48 h with pro-NGF (10 ng/ml; solid blue line), $PrP_{106–126}$ (10 µM; solid black line), or amyloid-$\beta_{1–40}$ (10 µM; dashed black line), in addition to increasing concentrations of EVT901 (from 0.01 to 100 nM). Apoptosis was measured and reported as % inhibition of apoptosis, representative of three independent experiments. (**H**) Induction of neuritogenesis through TrkA phosphorylation. SHSY-5Y cells serum-deprived, and treated with rhNGF (10 ng/ml) or EVT901 (0.01 to 10 nM), and then maintained in the same media for 3 days. The neurite length was visualized after staining with May-Grunwald-Giemsa and digitally photographed from randomly selected image fields (magnification × 10). (**I**) Confluent SHSY-5Y cells serum-deprived, and treated with NGF (10 ng/ml) or EVT901 (100 nM) for different times (1–3 days). Quantification of levels of total TrkA or phosphorylated TrkA (Tyr490) expressed as OD_{450} and representative of three independent experiments. Four-way ANOVA [time effect, $F(2,18) = 21.0$, $P < 0.001$; NGF effect, $F(1,18) = 152.75$, $P < 0.0001$; EVT901 effect, $F(1,18) = 4.32$, $P = 0.052$; pTrkA, not significant]. Note that there are significant interactions: time × NGF, $F(2,18) = 33.81$, $P < 0.0001$; time × EVT901, $F(2,8) = 40.19$, $P < 0.0001$; time × pTrkA, $F(2,18) = 5.99$, $P = 0.01$; NGF × pTrkA, $F(1,18) = 167.68$, $P = 0.0001$; EVT901 × pTrkA, $F(1,18) = 43.79$, $P = 0.00010$; time × NGF × pTrkA, $F(2,18) = 50.54$, $P = 0.0001$; time × EVT901 × pTrkA, $F(2,18) = 25.23$, $P = 0.0001$. $^{***}P < 0.001$ compared to untreated control. (**J**) Chemical structure of EVT901; 1-(phenyl-3, 6-dihydro-2H-pyridinyl)-2-(aryl-bridged piperazines)-ethanone.

Caspase activity assays

To detect apoptotic cell death, caspase activity was measured using a pan-caspase apoptotic detection kit (Carboxylflurorescein FLICA; Immunochemistry Technologies, LLC) according to the manufacturer's protocol. Briefly, after treating cells with proNGF and EVT901 for 24 h, cells were washed with PBS twice and then the 30 × FLICA solution was added to the medium at a 1:30 ratio. Cells were incubated for 1 h at 37 °C/5% CO_2 incubator, and protected from light. After washing cells twice with wash buffer, cells were fixed with 4% paraformaldehyde for 20 min. After washing with PBS, cells were mounted on slides containing a drop of mounting media (ProLong® Gold with DAPI, Invitrogen). The mounted cells were observed under a fluorescence microscope (Nikon) equipped with a digital camera (AxioCam, Zeiss) with 20 × objective and pictures taken in five different areas that contained ⩾100 DAPI-positive cells. Double positive cells and DAPI-positive cells were counted. Data were expressed as a percentage of double-positive cells against DAPI-positive cells: % positive cells = (number of double-positive cells/DAPI-positive cells × 100). Data were collected from three independent experiments.

Determination of p75NTR expression in oligodendrocyte precursor/oligodendrocyte cells

Cells were fixed with 4% paraformaldehyde for 20 min and then washed with PBS and treated with blocking buffer (10% goat serum/0.1% BSA/0.01% Triton™ X-100) for 1 h at room temperature. Anti-rabbit p75NTR Ab (1:1000 dilution; COVANCE) was added and incubated overnight at 4 °C. For negative controls, no antibody was added. After washing cells with PBS three times, secondary antibody (goat anti-rabbit Alexa 488, 1:200, Molecular Probes) was added and incubated for 1 h at room temperature. Cells were washed with PBS three times and cover-slipped with mounting media (ProLong® Gold with DAPI, Invitrogen). The mounted cells were observed under a fluorescence microscope (Nikon) equipped with a digital camera (AxioCam, Zeiss) with a 20 × objective and pictures were taken in five different areas containing > 100 DAPI-positive cells. Double-positive cells and DAPI-positive cells were counted, and data were expressed % double-positive cells versus DAPI-positive cells (number of double positive cells/DAPI positive cells × 100). Negative controls were stained with only secondary antibody. Data were collected from three independent experiments.

CCI-TBI and drug treatment

To generate the TBI, a controlled cortical impactor (Custom Design & Fabrication) was used as described previously (Inoue *et al.*, 2013). Surgical procedures were carried out aseptically under anaesthesia induced and maintained by 2–3% of isoflurane. The toe pinch-reflex test was used to determine the effectiveness of the anaesthetic prior to surgery. Lacri-Lube® ophthalmic ointment (Allergan Pharmaceuticals) was applied to the eyes prior to surgery. Body temperature was monitored using a rectal thermal probe and maintained at 37.5 ± 0.5 °C using a heating pad. Animals were administered 25 mg/kg of cefazolin (Ancef, Novation, LCC) prior to surgery and for 3 days postoperatively. Rats were mounted in a Kopf stereotaxic frame under isoflurane anaesthesia and maintained at 37.5 °C. A unilateral craniectomy was produced in the skull using a 6-mm diameter trephine positioned from 3 mm anterior to 3 mm posterior to bregma, and between 1.0 mm and 7.0 mm laterally from bregma. Moderate contusion brain injury was generated using the CCI device with a 5 mm diameter impactor tip positioned perpendicular to the surface, of the left somato-motor cortex, using a 2.0 mm displacement at 4 m/s velocity, and a dwell time of 150 ms. The injury sites were closed and the animals were recovered in a Thermocare® Intensive Care Unit with Dome Cover (Thermocare, Inclined Village). Sham-injury controls had all procedures including the craniectomy but without cortical contusion.

To infuse EVT901, rats had a jugular vein catheter placed under anaesthesia. Animals were placed in a supine position, a longitudinal cut was made in the skin, and muscles were retracted to expose the left jugular vein. Polyethylene tubing (0.58 mm internal diameter × 0.96 mm outer diameter; BPE-T50 Solomon Scientific) cut to a length of 12.5 cm was used to introduce drugs (vehicle or EVT901) into the vascular system. A 1.5 cm portion of the tubing was inserted into the jugular vein, secured using a 4.0 silk suture and fed subcutaneously to the back of the animal, allowing easy access for repeated drug administration. EVT901 doses (0, 1, 3, and 10 mg/kg) were prepared and labelled to allow for blinding of the investigators administering the drugs. The code used for each group was revealed at the end of the study. The total volume of solution was determined by the weight of each rat. Five mg/kg (v/w) of prepared EVT901 (or vehicle) was infused over 2 min via an infusion pump (BS-300 Syringe Infusion Pump, Braintree Scientific). EVT901 was infused once per day for 7 days starting at 4 h post-injury. Blood was collected by tail vein within 15 min of the initial infusion on Day 1 and the final infusion on Day 7 to confirm infusion of EVT901. Approximately 60 µl of blood was blotted on 903 protein saver cards (Whatman) and dried at room temperature. Analysis of the coded blood spots showed that each drug treatment level resulted in the predicted blood levels (not shown). Sample size was determined by power calculations based on previous studies (Inoue *et al.*, 2013) (n = 8–12 per group). Only data from animals surviving for the entire test period were included in the statistical analysis. Overall survival rate was 90%.

Western blot analysis of CCI-TBI tissue

Rats were perfused with PBS at 1, 2, 8, and 14 days post-injury. Brains were removed and the white matter region, cortex, and hippocampus were dissected for protein preparation. The tissue was homogenized in protein lysis buffer (1:5 ratio, Pierce IP Lysis buffer, Thermoscientific) including proteinase/phosphate inhibitor (Halt™ Protease and Phosphatase inhibitor cocktail, Thermoscientific), 5 mM EDTA and 1 mM PMSF and sonicated at 40 amplitude, 10 s pulse, two times. Protein lysate was obtained by centrifugation at 13 000 rcf for 10 min at 4 °C. Protein concentration was determined by the BCA protein assay kit (Pierce). Twenty micrograms of protein was added with Laemmli sample

buffer (Bio-Rad) including 20 mM DTT and β-mercaptoethanol and boiled for 5 min. Protein was loaded onto 4–20% tricine gel (Bio-Rad), electrophoresed, and transferred onto a PVDF membrane. After blocking the membrane with blocking buffer (Li-COR Bioscience), the membrane was incubated overnight at 4 °C with antibodies directed against p75NTR (1:1000, COVANCE, Cat #. PRB-602C), proNGF (1:500, Millipore, Cat #. AB9040), Cleaved caspase-3 (1:1000, Cell Signaling, Cat #. 9664), and β-actin (1:2500, Sigma). Membranes were washed three times for 5 min with PBS, secondary antibodies (anti-rabbit IR680 and/or anti-mouse IR800, 1:5000) were added and incubated for 1 h at room temperature. After washing membranes with PBS three times for 5 min, membranes were scanned with an Odyssey scanner (Li-COR Bioscience). Quantification was performed using the Odyssey scanner software (Li-COR Bioscience). β-Actin served as a loading control. The sample size was chosen based on preliminary data ($n = 3$ per group).

Histology, immunocytochemistry and cell counts for CCI-TBI animals

Rats were killed at 24 h or 8 days post-injury and transcardially perfused with PBS, followed by 4% paraformaldehyde. Brains were removed, post-fixed, and cryoprotected in 30% sucrose. Sections of 30 µm were cut on a cryostat (Microm). Sections were treated with blocking buffer (10% goat serum/0.1% BSA/0.01% Triton™ X-100) for 1 h at room temperature and stained overnight at 4 °C with antibodies against p75NTR (1:200, COVANCE, Cat #PRB-602C), proNGF (1:100, Millipore, Cat #AB9040), cleaved caspase-3 (1:100, Cell Signaling, Cat #9664), APC (1:10, Millipore, Cat #Ab16794), GFAP (1:100, Millipore, Cat #345860), and CD11b (1:100, Serotec, Cat #MCA275R). After washing with PBS three times, secondary antibodies (1:200; anti-rabbit Alexa 488; Molecular Probes, 1:200; anti-mouse Alexa 594; Molecular Probes) were added and incubated for 1 h at room temperature. Slides were washed with PBS three times for 5 min, and were mounted with mounting media (ProLong® Gold with DAPI, Invitrogen). Slides were analysed using a fluorescence microscope (Nikon) and images were captures with a digital camera (AxioCam, Zeiss).

Volumetric analysis

The Cavalieri probe method

To determine if EVT901 affects tissue damage after TBI, the estimated volume of the injured brain (including the 5 mm injured zone) was measured by systematic volumetric analysis. Briefly, at 8 days after TBI, the brains of paraformaldehyde perfused animals were collected and cut at 30 µm as described above. For each rat, 15 brain tissue sections (every 10 sections between +2.2 and −2.2 mm from Bregma) were chosen for stereological analysis and stained with Cresyl violet (Fig. 4D). The Cavalieri principle was used to generate unbiased estimates of volume using Stereo Investigator software (MBF Bioscience). As a Cavalieri probe, a 200-µm square grid was placed over the brain tissue section and all the grid points that overlay the areas of interest were marked. Areas included the hemisphere (Fig. 4B), cerebral cortex (Fig. 4C), and the white matter including the corpus callosum (Fig. 4C). All 15 brain tissue sections were evaluated by marking the grid points, which generate unbiased estimations of area. The volume was estimated by summing the areas and multiplying by the tissue thickness using Stereo Investigator software. Gunderson coefficient of error, m = 1, was evaluated to determine the accuracy of the stereological estimation and was < 0.05 (not shown) in this study ($n = 8$–12 per group). Sample size was determined by power calculations based on previous studies (Inoue *et al.*, 2013) ($n = 8$–12 per group).

Stereological analysis

Counting APC-positive cells

To determine if EVT901 protects oligodendrocytes from TBI, we quantify the number of oligodendrocytes in the white matter by unbiased stereological assessment. Briefly, a total of 10 brain sections were chosen for stereological analysis (every 330 µm interval between 1.5 mm anterior to 1.5 mm posterior to Bregma). Free-floating brain sections were stained with anti-CC1 antibody (APC clone) (1:100 dilution; Abcam, Cat #Ab16794) overnight at 4 °C. After washing with PBS, tissues were incubated with biotinylated antibody (VECSTAIN Elite ABC Kit, Vector Laboratories) for 30 min and visualized by 3,3' diaminobenzidine (DAB) chromogen (ImmPACT™ DAB Peroxidase substrate, VECTOR Laboratories). To quantify the number of APC-positive cells for unbiased assessment, systematic random sampling using the optical fractionator method in the region of interest was performed with Stereo Investigator (Fig. 4C). The white matter was contoured with a 2× objective and cells counted with a 63× objective. A counting grid was set as 245 µm × 183 µm and placed randomly over the contoured white matter (Zhao *et al.*, 2011). The counting frame was set as 30 µm × 30 µm with 3 µm guard zone (Lotocki *et al.*, 2011). Section thickness was measured at each counting site and the average tissue thickness was computed for stereological calculation by Stereo Investigator software. Average of tissue thickness was 18.95 ± 0.45 µm (SEM). The total number of CC1-positive cells was automatically calculated by Stereo Investigator using the following equation: $N = Q^- \times 1/\text{ssf} \times 1/\text{asf} \times 1/\text{hsf}$ (N is total neuron number, Q^- is the number of neurons counted, ssf is section sampling fraction, asf is the area sampling fraction, and hsf is the height sampling fraction). Coefficient of error, m = 1, was evaluated to determine the precision of the estimation of the stereological measurement. All Coefficients of error, m = 1, in each group was < 0.05 (not shown; $n = 5$–7 per group).

Counting NeuN-positive cells

To determine if EVT901 preserves neuronal cells from TBI, we quantified the number of NeuN-positive cell in the cerebral cortex by unbiased stereological assessment. Briefly, seven brain sections were chosen for stereological analysis (every 330 µm interval from between bregma levels +1.2 and −1.2 mm). Free-floating brain sections were stained with anti-NeuN antibody (1:100 dilution; Millipore, Cat #ABN90) overnight at 4 °C. After washing with PBS, tissues were incubated with biotinylated antibody (VECSTAIN Elite ABC Kit, Vector Laboratories) for 30 min and visualized by DAB chromogen (ImmPACT™ DAB Peroxidase substrate, VECTOR Laboratories). To quantify the number of NeuN-positive cells, the optical fractionator method

was used by Stereo Investigator. The rhinal fissure was used as a landmark to identify the lateral aspect of the neocortex (Fig. 4C) (Weskamp and Reichardt, 1991). The cortical region was contoured to the border of rhinal fissure with a 2× objective and counting was performed with 63× objective. The counting grid was set as 350 µm × 265 µm and placed randomly over the contoured cortical region (Weskamp and Reichardt, 1991). The counting frame was set as 50 µm × 50 µm with a 3 µm guard zone. The section thickness was measured at each counting site and the average tissue thickness was computed for stereological estimate calculation by Stereo Investigator software. Average tissue thickness was 19.02 ± 0.2675 µm (SEM). The total number of NeuN positive cells was automatically calculated by Stereo Investigator using the following equation: $N = Q^- \times 1/ssf \times 1/asf \times 1/hsf$ (N is total neuron number, Q^- is the number of neurons counted, ssf is section sampling fraction, asf is the area sampling fraction, and hsf is the height sampling fraction). Coefficient of error, m = 1, in this study was < 0.05 (data not shown; $n = 4$ per group).

Determination of myelin loss in white matter

To determine the effect of TBI on myelin loss, eriochrome cyanine was used for staining. Briefly, brain tissue sections were chosen from bregma −900 µm, where the most damaged white matter area based on unbiased systematic volumetric analysis using Cavalieri probe (Supplementary Fig. 2). After defatting with acetone, tissues were stained with eriochrome cyanine solution (0.3% eriochrome cyanine, 0.5% H_2SO_4, and 10% iron alum) for 30 min at room temperature in 5% iron alum solution until white matter (blue) was clearly differentiated from grey matter. Then tissue sections were placed in borax-ferricyanide solution (1% borax and 1.5% potassium ferricyanide) for 10 min to complete differentiation. After rinsing with water, tissues were dehydrated and mounted with DPX mounting media (Sigma). Entire brain tissue images were captured with ×10 magnification and stitched by BZ-8100 (BIOREVO microscope, Keyence). To measure intensity of eriochrome cyanine staining, NIH ImageJ software was used. Briefly, the entire brain images were opened with ImageJ software, converted to 8 bit image, and contoured white matter areas in ipsilateral and contralateral hemisphere were indicated as the region of interest. To obtain only myelin-positive signal, the image was adjusted using bright/contrast by setting threshold to the grey scale range of 70–250 (Image J > Image > adjust images). Then the region of interest was selected and the integrated density measured (Image J > Integrated density > analyze > measurement). The integrated density value for contralateral was used for the internal control. Data are presented as a percentage (intensity of ipsilateral/intensity of contralateral) × 100 ($n = 5$ per group). The sample size was chosen based on preliminary data ($n = 5$ per group).

Determination of microglia activation in white matter

To estimate microglial activation, we used a proportional area measurement modified from previous reports (Popovich *et al.*, 1999; Zhang *et al.*, 2011). Five brain tissue sections at 600-µm intervals from Bregma + 1.2 mm to −1.2 mm were measured from each rat. Briefly, brain tissue sections were treated with peroxidase block (Dako EnVision™ + System-HRP, DAKO) for 5 min, washed with PBS, and then incubated with CD-11b Ab (1:100 dilution, AbD Serotec, Cat #MCA275R) for 1 h at room temperature. After washing with PBS, peroxidase-labelled polymer (Dako EnVision + System-HRP, DAKO) was applied for 30 min at room temperature. Tissues were washed with PBS and then visualized with DAB chromogen for 10 min. The reaction was stopped with distilled water. The stained sections were observed on a Zeiss microscope. For assessing CD11b-positive cells in the white matter, two different areas (157.5 × 101.6 mm) in the ipsilateral and contralateral side of brain from the corpus callosum were photographed under a 40× objective using a digital camera (Retiga EXi Fast1394, Qimaging). To measure the proportional area of reactive microglia, we used threshold measurement by MetaMorph® software (Molecular Devices). Briefly, images were opened with MetaMorph® software and the intensity of the background was measured using 'Region Measurement'. Using 'Set Color Threshold', the threshold was set on the CD11b-positive signal, while the pre-measured background intensity was set as baseline (Metamorph > Set Color threshold). Once threshold was set, CD11b-positive signal was measured using Region Measurement. Data are presented as percentage (threshold area of CD11b-positive/total area) × 100 ($n = 5$ per group). The sample size was chosen based on preliminary data ($n = 5$ per group).

Behavioural evaluation for motor recovery

The paw placement test was performed as previously described (Inoue *et al.*, 2013). Briefly, rats were placed in a clear plastic cylinder. The spontaneous behaviour of the rats was recorded with a digital camera for 3 min, and the number of times the rat placed its left, right, or both forepaws against the cylinder during weight supported movements was determined. Individual placements were scored as 'left', 'right', or 'both'. Scoring was performed using video playback by two trained raters independently in a blinded manner. Rats were tested before surgery and on Days 2 and 7 after TBI. Sample size was determined by power calculations based on previous studies (Inoue *et al.*, 2013) ($n = 8$–12 per group).

Fluid percussion traumatic brain injury and outcome measures

Male Sprague Dawley rats (strain RjHan; Janvier) (170–230 g) were anaesthetized with sodium pentobarbital for trauma, placed in a stereotaxic frame, and a hole (4 mm in diameter) was made at the level of the right parietal cortex (the centre being located 3.5 mm posterior to bregma, 7 mm lateral to the midline and 3.5 mm below the upper surface of the skull). A 1.6 mm internal diameter Teflon tube was placed in contact with the dura and fixed into the craniotomy with dental acrylic cement. The tube was connected to a Beckman HPLC pump and was filled with sterile injectable water. An FPI of moderate intensity (5 bar) was induced by a brief opening of the electronically controlled solenoid valve (100 ms). Thereafter, the tubing was removed, the scalp sutured and animals placed

under a heating lamp for recovery from anaesthesia. The mortality rate was ~5%. The severity of injury was confirmed by assessing cognitive deficits. Sham rats were surgically prepared in the same manner but did not undergo craniotomy. EVT901 or its vehicle was administered orally by intragastric gavage (5 ml/kg in a solution of 0.6% methylcellulose/0.5% Tween 80), once a day, 24 h after the surgery, and for 23 days.

Behavioural evaluation of memory deficits

Object recognition test

Memory assessment was performed 5 days after the end of treatment on Day 28 post-injury. The test consisted of three sessions. The first session was for habituation (exploration for 3 min, record of the time spent in active movements). The second at 24 h later, was the acquisition session; the rat was placed in the box with two identical objects located in opposite corners, and the time to achieve 20 s exploring those two objects was recorded (limit of 6 min). Rats were replaced in the box 1 h later, for the third recall session of 5 min, with a previously presented familiar object and a novel object. Time spent exploring the familiar (F) and the novel (N) objects was recorded. Others parameters calculated from the recall session: total exploratory time (N + F) and the novelty index (N – F/N + F).

Conditioned freezing response test

Memory deficits were evaluated using the conditioned freezing response test. Rats were conditioned to associate the context with a foot shock, and then tested for fear-associated freezing to the context. Briefly, two sessions, 24 h apart were used. First, rats were introduced to the experimental box where they received a scrambled electric foot-shock (0.6 mA, 1.5 s). In the second session, the rats were replaced in the same box for 3 min, and the duration of freezing (complete lack of movement except for breathing) was recorded.

Behavioural evaluation of seizure susceptibility

Epileptogenesis

To detect any enhanced seizure susceptibility in post-TBI rats, a kainate sensitivity test was performed 42 days after the traumatic injury and 5 days after the last administration of the compound EVT901 (1 mg/kg/day, oral administration for 42 days). Evaluation of the increased susceptibility of rats to seizure induction by kainate was determined after a single injection of sub-convulsant dose of kainate (8 mg/kg, intraperitoneally). Movement was evaluated from 45 min to 3 h 45 min post-kainate injection: each rat was observed and convulsions were scored into five classes by a standard method (Racine's score) (from stage 1: immobility, to stage 5: forelimb clonus, rearing and loss of postural tone). For each group, a status epilepticus was defined, corresponding to the per cent of rats that reached continuous seizure activity in the different groups.

Immunohistochemistry

p75NTR and Fluoro-Jade® staining

Free-floating tissue sections were incubated overnight at 4 °C with anti-p75NTR antibody (1:1000, Millipore) in PBS-T/serum 1%, then with secondary antibody (Vector Vectastain ABC kit) and avidin-biotin-peroxidase complex (Vector Laboratories). Sections were visualized using a DAB substrate kit for peroxidase (DAB kit, DAKO), mounted on glass slides, air dried, alcohol dehydrated and cover-slipped with Eukitt® mounting medium (Eukitt EMS). For Fluoro-Jade® staining, tissue sections were directly mounted onto DAKO-Flex slides, hydrated and incubated in a solution of potassium permanganate. After incubation in a solution of Fluoro-Jade® B (Chemicon), sections were air-dried, immersed in xylene, cover-slipped as previously, and visualized using FITC fluorescence microscopy. Digital images were collected and Fluoro-Jade B-positive cells were subsequently counted using Explora Nova software; averages were used for statistical analysis.

Randomization and blinding

All animal studies were performed with randomized treatment allocation and outcomes assessed by experimenters blind to condition.

Statistical analysis

Analysis of all biochemical, histological and behavioural data was performed in SPSS v.19 (IBM) by an independent statistician. One-way, two-way (or higher order) balanced, factorial analysis of variance (ANOVA; SPSS General Linear Model command) was used to explicitly test each factor in the balanced factorial experimental designs. The statistical approach ensured two-tailed, balanced testing of main effects and interactions across all factorial combinations of treatments. Technical replicates and independent experiments were statistically treated as random effects, thereby correcting for technical variance to directly test treatment effects conserved across replicates. Comparison of two groups was performed by an unpaired, two-tailed Student's *t*-test. For behavioural analysis of cognitive/motor function, mixed factorial repeated measures ANOVA was used. Sample sizes (n) were justified by power calculations and all analytics were applied after checking for statistical assumptions (normality, homogeneity of variance, sphericity). Statistical significance was defined at $P \leqslant 0.05$. Data are expressed as means ± SEM. F-values and degrees of freedom are reported in figure legends.

Results

EVT901 inhibits p75NTR signalling, blocks apoptosis, and activates TrkA

To determine whether a small molecule could bind to p75NTR and disrupt the preassembly step (Chan, 2007), we set up a screen to detect protein/protein interaction with reliable quantification. The soluble truncated form of p75NTR, containing only the four CRDs fused to alkaline

phosphatase (AP-p75NTR), was used as ligand and probe to detect p75NTR oligomerization on SK-N-BE human neuroblastoma cells stably transfected with full length-p75NTR (SK-N-BE-p75NTR). More than 400 molecules, selected from a library of compounds active on a phenotypic model of neurogenesis, were screened for their ability to inhibit the pre-oligomerization of p75NTR (ligand-independent). Thus, a dedicated chemical program allowed us to select new leads characterized by aryl substituted piperazine and showing nanomolar activity. From the structure/activity relationship analysis, an oriented second back-screening campaign, in particular with introduction of bridged piperazines replacing the piperazine moiety, led us to select a new chemical series [1-(phenyl-3, 6-dihydro-2H-pyridinyl)-2-(aryl-bridged piperazines)-ethanone] with high potency, specificity and selectivity; those compounds were also screened *in vitro* to inhibit apoptosis in neuroblastoma cells. Through the optimization process, we identified EVT901 (Fig. 1J) as a highly active compound with sub-nanomolar potency; and a full characterization of its selectivity and ADME (absorption, distribution, metabolism and excretion) *in vitro* and *in vivo* properties was carried out. EVT901 showed a high ability to inhibit the binding of AP-p75NTR to p75NTR in a dose-dependent manner, with sub-nanomolar potency (IC_{50} of 0.21 ± 0.04 nM) (Fig. 1A). EVT901 also alters NGF binding to p75NTR (Fig. 1B).

To determine whether a specific self-association domain (PLAD) is present on the p75NTR and if EVT901 can interfere with its oligomerization (Chan *et al.*, 2000), we co-expressed full-length HA-p75NTR and Flag-p75NTR tagged receptors in HEK293T cells. High levels of Flag-p75NTR association with the HA-p75NTR were observed when both receptors were co-expressed, demonstrating that p75NTR is able to self-oligomerize independently of ligand binding (Fig. 1C). Interestingly, EVT901 dose-dependently reduced this association, suggesting that EVT901 can interfere with p75NTR pre-oligomerization. To confirm that EVT901 interferes directly at the level of a PLAD (Gentry *et al.*, 2004), we designed different mutated and chimeric receptors (Fig. 1E). Transfection efficiency of these chimeric receptors was confirmed using an anti-HA antibody to detect surface expression using flow cytometry. Expression of the various constructs was between 85% and 95% of cells (data not shown). Consistent with a previous study (Ye *et al.*, 1999), overexpression of full-length p75NTR induced spontaneous apoptosis, which was significantly abrogated by EVT901 at 100 nM (Fig. 1D). Overexpression of a deleted form of p75NTR (CRD1-p75NTR) also induced high levels of apoptosis, which was strongly reduced in the presence of EVT901. Moreover, EVT901 was not able to abrogate CD40-induced apoptosis, clearly suggesting its specificity for p75NTR. Although specific deletions may disrupt receptor structure, we generated a chimeric receptor by exchanging the first CRD of CD40 receptor with the CRD1 of p75NTR and confirmed that expression of this chimeric receptor on HEK cells induced strong spontaneous apoptosis, similar to wild-type cells (Fig. 1D and E). In this model, EVT901 showed anti-apoptotic activity confirming that the site of interaction of EVT901 is located on the CRD1 of p75NTR (Fig. 1D). The specificity of EVT901 to p75NTR versus other members of the TNFR superfamily (TNFR1, TNFR2, HVEM, 4-1BB, LTβR, DR5, BCMA, FAS) was further confirmed by demonstrating that EVT901 does not inhibit apoptosis of HEK293T cells induced by overexpression of these receptors (Fig. 1F). As a follow-up to the p75NTR-overexpression models, it was essential that EVT901 was also able to abrogate p75NTR signalling in a cell type expressing endogenous p75NTR. Therefore, we confirmed the neuroprotective effects of EVT901 on SH-SY5Y cells, where apoptosis is induced by pro-NGF (IC_{50} of 0.51 ± 0.16 nM) (Fig. 1G).

Well known to exhibit prevalent β-sheet structures and to form fibrillar aggregates, the prion protein ($PrP_{106–126}$) and amyloid (amyloid-$\beta_{1–40}$) peptides induce pro-apoptotic signalling via p75NTR. We hypothesized that the interaction site(s) of these peptides on p75NTR are different from that of the neurotrophins, and could be located in the CRD1 domain of p75NTR. We first evaluated the effect of these two aggregated peptides on apoptosis in SH-SY5Y cells. Incubation with $PrP_{106–126}$, or amyloid-$\beta_{1–40}$, increased cell death (not shown). Interestingly, EVT901 was able to strongly reverse apoptosis induced by these two aggregated peptides with IC_{50s} of 0.69 ± 0.30 nM for $PrP_{106–126}$ and 0.42 ± 0.11 nM for amyloid-$\beta_{1–40}$ (Fig. 1G). Moreover, the potency of EVT901 against apoptosis induced by these peptides suggests that the functional epitope on p75NTR interacting with $PrP_{106–126}$ and amyloid-$\beta_{1–40}$, is located on the CRD1 domain. This hypothesis was further supported by the pro-apoptotic efficacy of these peptides on the short form of p75NTR containing only CRD1 in the extracellular part.

Previous findings suggest p75NTR mediates NGF-induced neuronal cell survival and neurite outgrowth by regulating the TrkA-mediated signalling pathway. We tested whether EVT901 interferes with TrkA-dependent neurite outgrowth on SH-SY5Y cells expressing both TrkA and p75NTR. Increasing concentrations of EVT901 induced extensive neuritogenesis in a dose-dependent manner, as compared to untreated controls (Fig. 1H), suggesting that EVT901 can modulate TrkA activation by facilitating the interaction of p75NTR monomers with TrkA. To further validate this hypothesis, we showed that the level of TrkA phosphorylation is strongly increased by stimulation with rhNGF (Fig. 1I), and EVT901 dramatically increased TrkA phosphorylation after 3 days of treatment, correlating with the induction of neurite outgrowth (Fig. 1I).

ProNGF has been shown to induce caspase activation and apoptosis in cultured oligodendrocytes via p75NTR (Beattie *et al.*, 2002). Here we tested if EVT901 would reduce this pro-NGF-induced apoptosis in mature oligodendrocytes and OPCs in culture, and show that adding

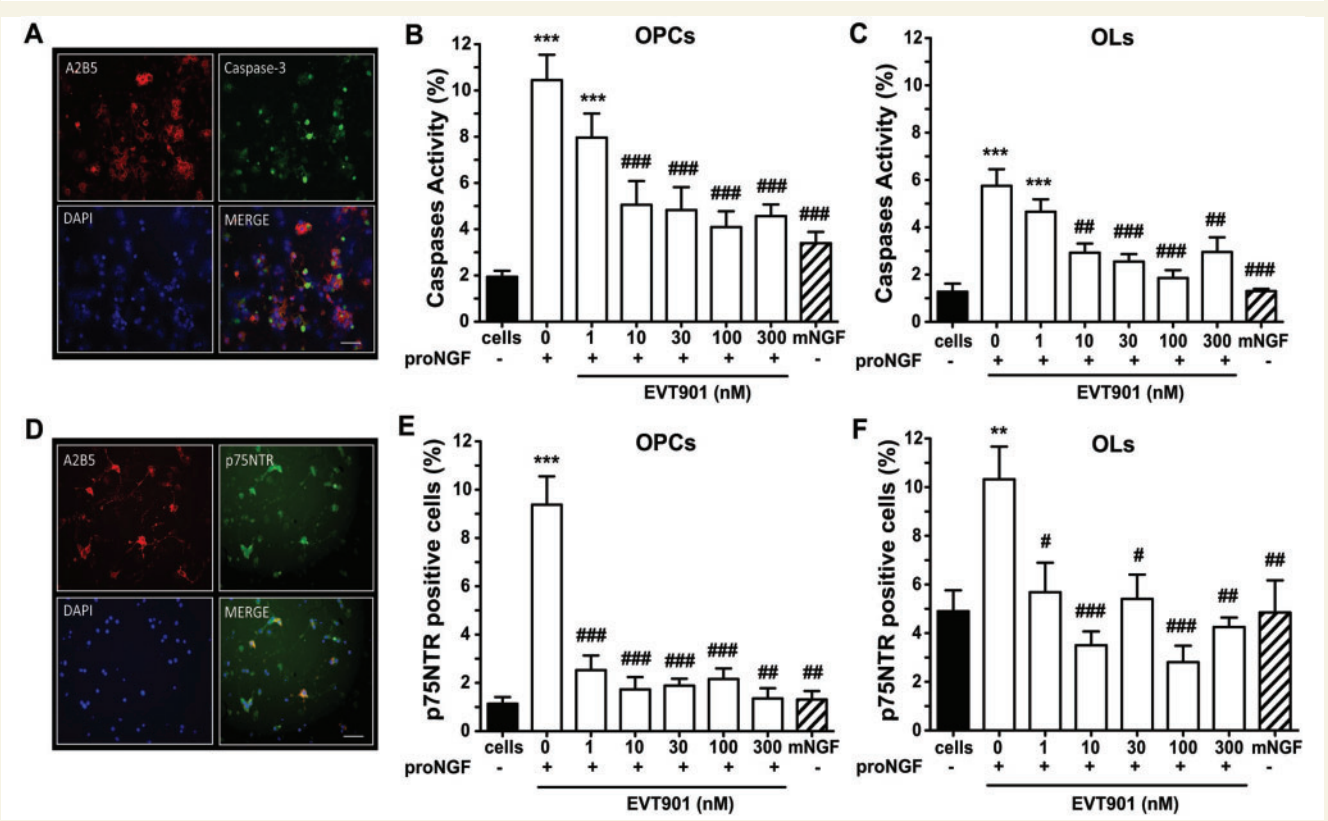

Figure 2 EVT901 blocks proNGF-mediated caspase activity and p75NTR expression in OPCs and oligodendrocytes *in vitro* and reduces proNGF-induced cell death. (**A**) Immunostaining showed that treatment with pro-NGF (50 ng/ml) induced caspase-3 activity in OPCs *in vitro*. (**B** and **C**) Caspase activity was measured by counting positive cells using the FLICA assay. Pro-NGF (50 ng/ml) increased caspase activity in cultured OPCs and oligodendrocytes. However, EVT901 added to the medium reduced the percentage of caspase-positive cells in a dose-dependent manner for OPCs and oligodendrocytes [one-way ANOVA, $F(7,67) = 10.02$, $P < 0.0001$ for OPCs and $F(7,65) = 10.55$, $P < 0.0001$ for oligodendrocytes]. (**D–F**) Both OPCs and oligodendrocytes expressed p75NTR in a small percentage of cells *in vitro*, this was increased significantly by the addition of pro-NGF, and co-incubation with EVT901 reduced or inhibited p75NTR expression. Note that mature NGF (mNGF) had no effect on apoptosis or p75NTR expression. One-way ANOVA, $F(7,105) = 20.30$, $P < 0.0001$ and $F(7,98) = 5.68$, $P < 0.0001$ for OPCs and oligodendrocytes, respectively. $^{***}P < 0.0001$ compared to cells alone; $^{\#}P < 0.05$, $^{\#\#}P < 0.005$, $^{\#\#\#}P < 0.0001$ compared to 0 nM EVT901. Scale bar = 30 μm.

proNGF for 24 h increased p75NTR expression and caspase activation, and a wide dosing range of EVT901 inhibited both (Fig. 2). Thus, EVT901 may provide protection from proNGF toxicity by both reducing expression of p75NTR and by blocking proNGF-induced p75NTR oligomerization and apoptotic signalling.

EVT901 is protective in a unilateral CCI-TBI model and improves outcomes

CCI-TBI transiently increased p75NTR protein level at 1 and 2 days post-injury in the ipsilateral white matter (Fig. 3A and B). Immuno-staining revealed that p75NTR was co-localized in CC1 positive cells at 24 h following CCI-TBI, suggesting that injury induces p75NTR-expression in oligodendrocytes, as reported after spinal cord injury (Beattie *et al.*, 2002) (Fig. 3B). p75NTR was not co-localized in GFAP + astrocytes (not shown). Western blot analysis showed a rapid (and longer) transient increase in proNGF after TBI, returning to normal at 14 days (Fig. 3C) and this could induce apoptosis in oligodendrocytes in the subcortical white matter. Indeed, western blots using an antibody to cleaved caspase-3 revealed a significant increase in expression by 8 days after TBI (Fig. 3E), similar to that seen in the dorsal columns after spinal cord injury (Beattie *et al.*, 2002; Sun *et al.*, 2010). Evidence for co-localization of CC1 and cleaved caspase-3 in immunostained sections was seen as early as 1 day post-TBI (Fig. 3F). In addition, p75NTR protein levels were significantly increased in both cortex after TBI (Supplementary Fig. 1), suggesting that p75NTR is also involved in neuronal cell death *in vivo*.

Cerebral, cortical, and subcortical white matter volumes, measured using unbiased stereological methods at 8 days post-TBI (Fig. 4), were significantly reduced by TBI, and EVT901 dose-dependently mitigated the loss (Fig. 4F, G and Supplementary Fig. 2A and B). Using stereological estimates of oligodendrocytes in the subcortical white matter

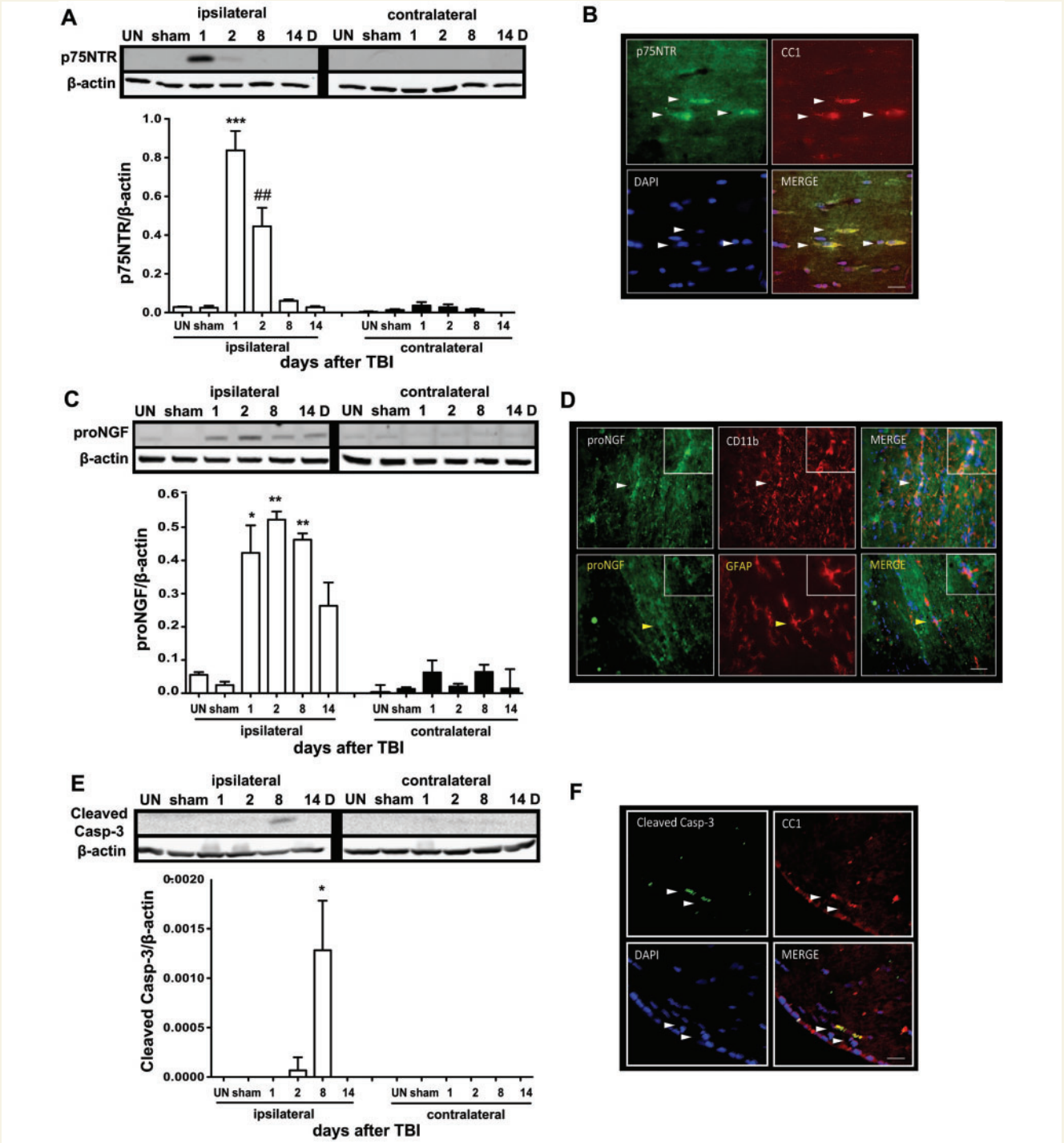

Figure 3 Induction of p75NTR and proNGF in the white matter (corpus callosum) after CCI-TBI. (**A–D**) Immunoblot analysis showed that both p75NTR and proNGF protein levels are increased after TBI in the ipsilateral white matter as compared to uninjured (UN) and sham injured tissue. Two-way ANOVA, (**A**) for p75NTR: side, $F(1,12) = 92.42$, $P < 0.0001$; time, $F(5,12) = 32.32$, $P < 0.0001$; (**C**) for proNGF: side, $F(1,12) = 126.54$, $P < 0.0001$; time, $F(5,12) = 18.18$, $P < 0.001$. In ipsilateral white matter, p75NTR and proNGF are significantly increased [$F(5,12) = 32.55$, $P < 0.0001$ and $F(5,12) = 11.72$, $P < 0.0001$, respectively]. (**B**) P75NTR immunoreactivity is co-localized with CC1 expression in cells with oligodendrocyte morphologies (arrowheads). Scale bar = 20 μm. (**D**) ProNGF immunoreactivity is co-localized in CD11b-positive and GFAP-positive cells (arrowheads), suggesting that microglia and astrocytes are responsible for proNGF expression in the corpus callosum at 1 day after TBI. Scale bars = 50 μm. (**E**) Immunoblot analysis showed that TBI increased the cleaved caspase-3 expression on the ipsilateral side compared to the contralateral side at 8 days after injury [side, $F(1,12) = 6.78$, $P < 0.05$; time, $F(5,12) = 6.02$, $P < 0.01$]. In the ipsilateral white matter, cleaved caspase-3 protein level is significantly increased [$F(5,12) = 6.02$, $P < 0.01$]. $^{*}P < 0.05$, $^{**}P < 0.005$, $^{***}P < 0.0005$, $^{\#\#}P < 0.01$ compared to sham; $n = 3$/group; Error bars indicate ±SEM. (**F**) Cleaved caspase-3 immunoreactivity is co-localized in CC1 positive oligodendrocytes (arrowheads). Scale bar = 50 μm. $^{*}P < 0.05$, $^{**}P < 0.005$, $^{***}P < 0.0005$, $^{\#\#}P < 0.01$ compared to sham.

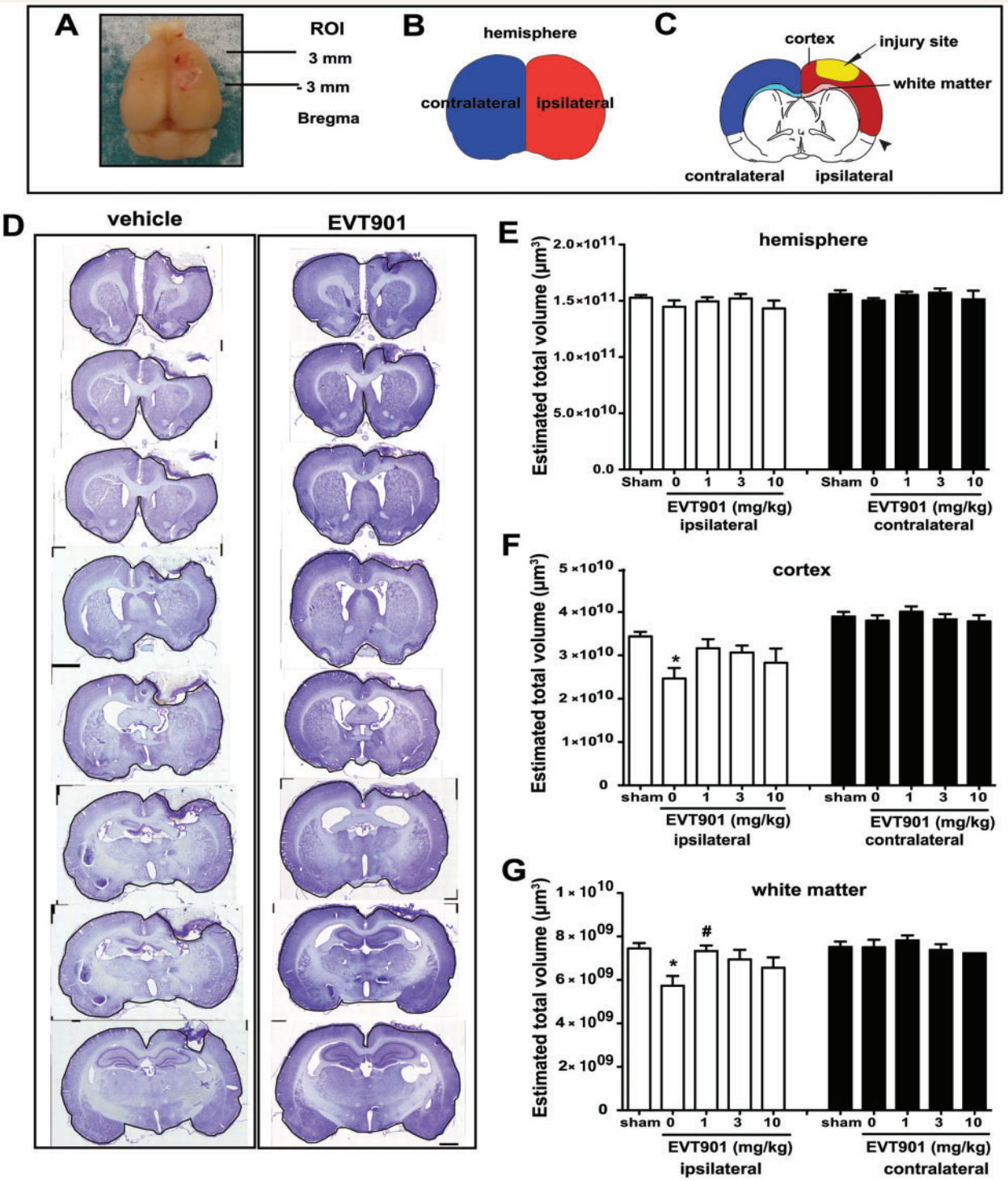

Figure 4 EVT901 treatment reduced atrophy in grey and white matter at 8 days post injury. (**A**) The region of interest (ROI) included tissue from 3 mm anterior to 3 mm posterior to bregma. (**B** and **C**) Illustration of representative brain figures of the hemisphere (**B**) and cerebral cortex and white matter (**C**), where stereological methods were used to estimate tissue volume by counting Cavalieri markers using Stereo Investigator. (**C**) The region of interest included the cerebral cortex from the midline to the rhinal fissure (small arrowhead); the ipsilateral cerebral cortex is indicated in red versus the contralateral cerebral cortex in blue, and ipsilateral white matter is indicated in pink whereas light blue indicates contralateral white matter. (**D**) Representative brain tissues stained with Cresyl Violet. Scale bar = 1 mm. (**E**) Total estimated volume was measured in each hemisphere. Total volume did not change between the ipsilateral and contralateral hemispheres at 8 days post-injury. (**F**) Total cortical volume estimates revealed significant atrophy of cortex on the ipsilateral but not contralateral side after TBI [two-way ANOVA, side, $F(1,45) = 101.09$, $P < 0.001$]; $^{*}P < 0.05$ compared to sham. However, EVT901 treatment was protective on the ipsilateral side [dose × side, $F(4,45) = 2.69$, $P < 0.05$]; $n = 8$–12 per group. (**G**) Total white matter volume was also significantly reduced ipsilateral to the injury [side effect, $F(1,45) = 17.51$, $P < 0.001$; dose effect, $F(4,45) = 2.22$, $P > 0.05$]. EVT901 treatment preserved white matter volume on the ipsilateral side [side × dose, $F(4,45) = 2.98$, $P < 0.05$]. $^{*}P < 0.05$ compared to sham, $^{\#}P < 0.05$ compared to 0 mg/kg. Error bar indicates ± SEM.

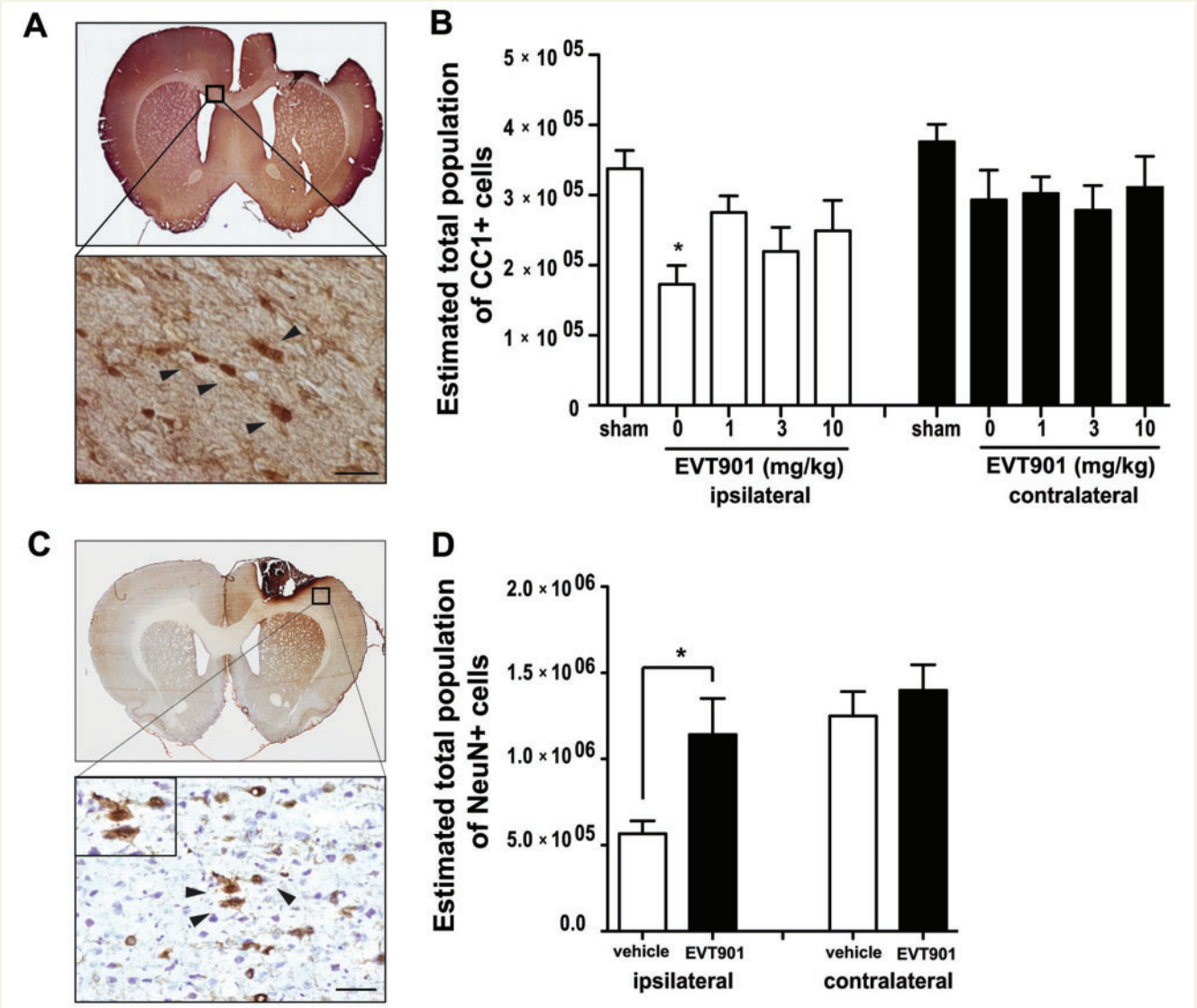

Figure 5 EVT901 treatment inhibits cell death in the cerebral cortex and underlying white matter at 8 days after CCI-TBI. (**A**) Stereological sampling of total number of oligodendrocytes (CC1-positive cells, arrowheads in the inset) in white matter was evaluated on DAB immunostained sections. (**B**) Cell numbers were estimated using unbiased stereology by optical fractionation (see 'Materials and methods' section; Stereo Investigator). TBI significantly reduced the number of CC1-positive cells in the white matter ipsilateral to the TBI. Two-way ANOVA, side, $F(1,28) = 17.51$, $P < 0.0001$. EVT901 treatment preserved the number of oligodendrocytes ipsilateral to the lesion [dose × side, $F(4,28) = 2.69$, $P = 0.05$]. $n = 5$–7 per group. Error bar indicates ± SEM. A subsequent t-test showed a significant difference between 0 and 1 mg/kg on the ipsilateral side ($P < 0.05$). (**C**) Neuronal loss was evaluated in sections immunostained for NeuN using DAB; cell staining in the ipsilateral perilesional cortex is shown for representative vehicle and EVT901-treated cases. Arrows indicate individual neurons. (**D**) Unbiased stereological analysis by optical fractionation was used to count NeuN-positive cells (see 'Materials and methods' section; Stereo Investigator). TBI caused a marked reduction in the number of cortical neurons counted ispilaterally versus contralaterally. Two-way ANOVA, side, $F(1,6) = 28.65$, $P < 0.01$. However, EVT901 treatment (1 mg/kg) protects NeuN-positive cells on the ipsilateral side [$F(1,6) = 5.89$, $P = 0.05$]. $^*P < 0.05$ compared to vehicle, $n = 5$. Scale bar = 10 μm.

(Fig. 5A and B), TBI significantly reduced CC1-positive oligodendrocytes and EVT901 treatments partially prevented this loss. Stereological counts of spared NeuN-positive cells in the cortical lesion area showed significant loss after TBI, and a protection after EVT901 treatment (Fig. 5C and D). Further, EVT901 treatment preserved myelin when compared to vehicle controls (Fig. 6A and B).

Using OX-42 staining density as a measure of microglial activation in tissue sections from vehicle and EVT901-treated (1 mg/kg) animals (Fig. 6C and D), EVT901 reduced microglial activation. Microglial activation has been shown previously to be associated with the loss of CC1 positive oligodendrocytes by apoptosis (Shuman *et al.*, 1997; Sun *et al.*, 2010).

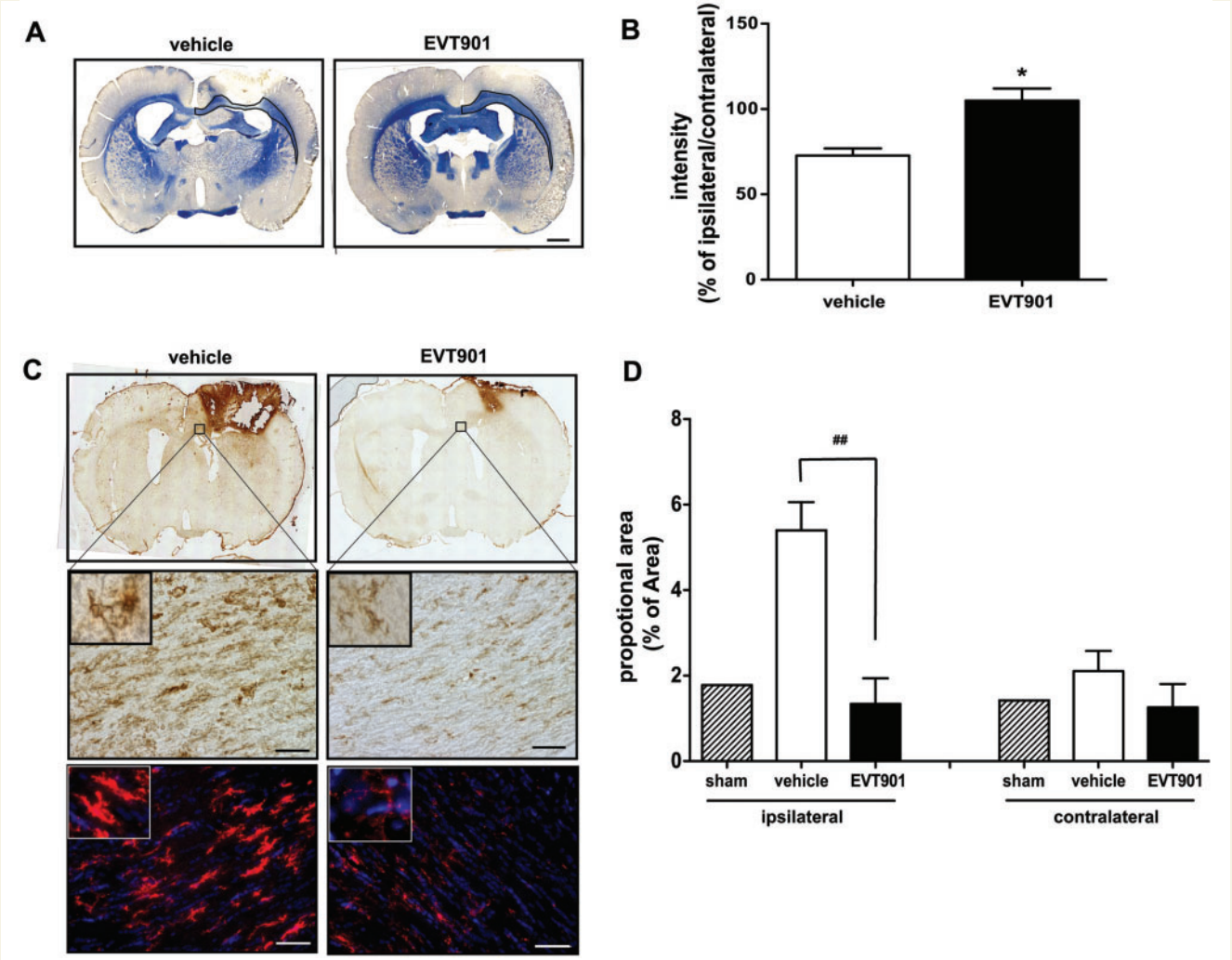

Figure 6 EVT901 treatment spares myelin and reduces microglial activation at 8 days after CCI-TBI. (**A** and **B**) Eriochrome cyanine staining showed a dramatic loss of myelin staining after CCI-TBI that was significantly reversed by 7 days of EVT901 treatment (1 mg/kg). Intensity measurements of staining in the white matter (outlined area) ipsilateral to the injury as a proportion of the same area on the contralateral side, revealed a significant effect of EVT901 treatment. n = 3–5/group. Two tailed t-test, $^{*}P < 0.05$. Scale bar in **A** = 1 mm. (**C**) Brain tissue sections were immuno-stained with OX-42 to reveal the presence of microglia. Representative sections showing staining in the corpus callosum are shown for vehicle and EVT901-treated (1 mg/kg) subjects. Both DAB (*middle*) and fluorescent (OX-42 in red, DAPI in blue) immunostained sections are shown. Scale bars = 50 μm. (**D**) Microglial activation, measured by proportional area of OX-42 staining, was increased ipsilateral to the lesion; EVT901 treatment reduced OX-42 staining [two way ANOVA, side, $F(1,8) = 44.96$, $P < 0.002$; dose, $F(1,18) = 10.11$, $P < 0.05$]. There was also a significant dose × side interaction in microglia activation with EVT901 treatment [$F(1,8) = 40.85$, $P < 0.001$]. $^{\#\#}P < 0.01$ compared to vehicle; n = 3–5/group. Bars represent mean ± SEM.

Paw use for exploration in a cylinder is significantly reduced on the side contralateral to a cortical injury (Inoue *et al.*, 2013). This was also partially preserved by EVT901 treatment (Supplementary Fig. 2E).

Oral EVT901 improves long-term outcomes in another TBI model

The results of our CCI-TBI studies provide evidence for a neuroprotective effect of EVT901 when the drug is given intravenously over 7 days; there is a clear positive effect on oligodendrocytes and white matter integrity, neuronal protection, and at least one sensorimotor function test. To examine the generality and persistence of these results, EVT901 was administered over a longer time course in another TBI model where trauma is induced by a focal lateral fluid percussion injury of the parietal cortex (FPI-TBI).

Similar to the effects of CCI-TBI, FPI-TBI produced an early expression of p75NTR at 1–2 days post-injury in the dentate gyrus, a structure where damaged neurons were also observed (Fig. 7A and B). Particularly vulnerable to FPI-TBI, the thalamus manifested marked positive Fluoro-Jade® staining at 14 days post-TBI (Fig. 7C). EVT901 significantly decreased Fluoro-Jade®-positive cells

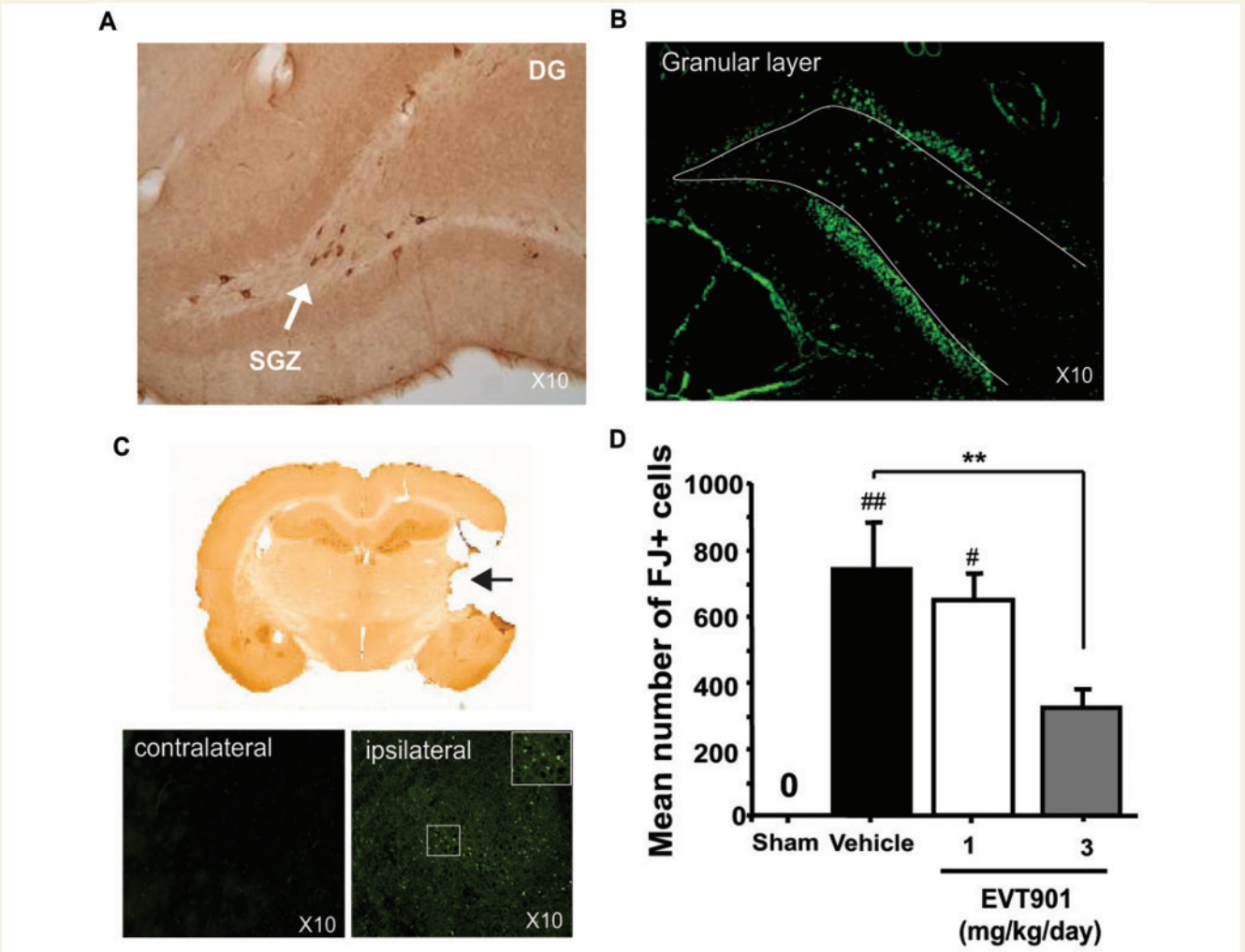

Figure 7 Acute expression of p75NTR after FPI-TBI and reduction of neurodegeneration with EVT901 *in vivo*. (**A**) Immunohistochemical expression of p75NTR at 1–2 days in the dentate gyrus of TBI rats using specific anti-p75NTR antibody. (**B**) Representative photomicrographs (original magnification × 10) of Fluoro-Jade® staining of damaged neurons in the granular layer of the dentate gyrus in FPI-TBI rats 1 week post-injury. (**C**) Representative photomicrographs of Fluoro-Jade®-stained sections from the thalamus 14-days post-trauma (ipsilateral versus contralateral to the injury). (**D**) Quantification of Fluoro-Jade® B-positive degenerating cells in the thalamus of FPI-TBI rats after EVT901 treatment. Following Fluoro-Jade staining, the digital images were collected and the damaged cells were quantified using Explora Nova Software. Three mg/kg/day of EVT901 protected neurons in the thalamus after TBI [one-way ANOVA, EVT901 effect, $F(3,18) = 8.46$, $P = 0.001$]. $^{\#}P < 0.05$ and $^{\#\#}P < 0.005$ compared to sham. $^{**}P < 0.01$ compared to vehicle. $n = 5$–7/group. Bars represent mean ± SEM.

(324.3 ± 54.1 cells) in the dorsal thalamus on the injured side as compared to the vehicle (741.8 ± 138.4 cells) (Fig. 7D).

Furthermore, EVT901 administered orally beginning at 24 h and then daily for 23 days, dose-dependently restored object recognition performance and significantly improved the ability of rats to discriminate between objects compared to sham-treated animals (Fig. 8A–C). Time spent by treated rats on novel versus the familiar objects was significantly and dose-dependently increased at 1 and 3 mg/kg/day, and full recovery was observed after 23 days exposure (Fig. 8A and B). There was a significant increase in the novelty index, as reflected by total exploration time (Fig. 8C). FPI-TBI induced a 75% reduction in the freezing response compared to sham; EVT901 significantly reinstated freezing durations at 0.3 and 1 mg/kg/day (84% and 88% recovery, respectively) (Fig. 8D). These studies suggest that EVT901 abrogates memory deficit induced by FPI-TBI.

TBI has been associated with increased seizure activity, so the effect of EVT901 treatment on hypersensitivity to a pro-convulsive agent was evaluated. Six weeks after injury, a subconvulsive dose of kainate elicits full-blown generalized tonic-clonic seizures (status epilepticus) in 90% of the rats with TBI (Fig. 8F). EVT901 treatment significantly decreased the intensity of post-TBI seizures (Fig. 8E), as well as the susceptibility to post-TBI seizures (Fig. 8F), further reinforcing EVT901's pharmacological potential for treating CNS trauma.

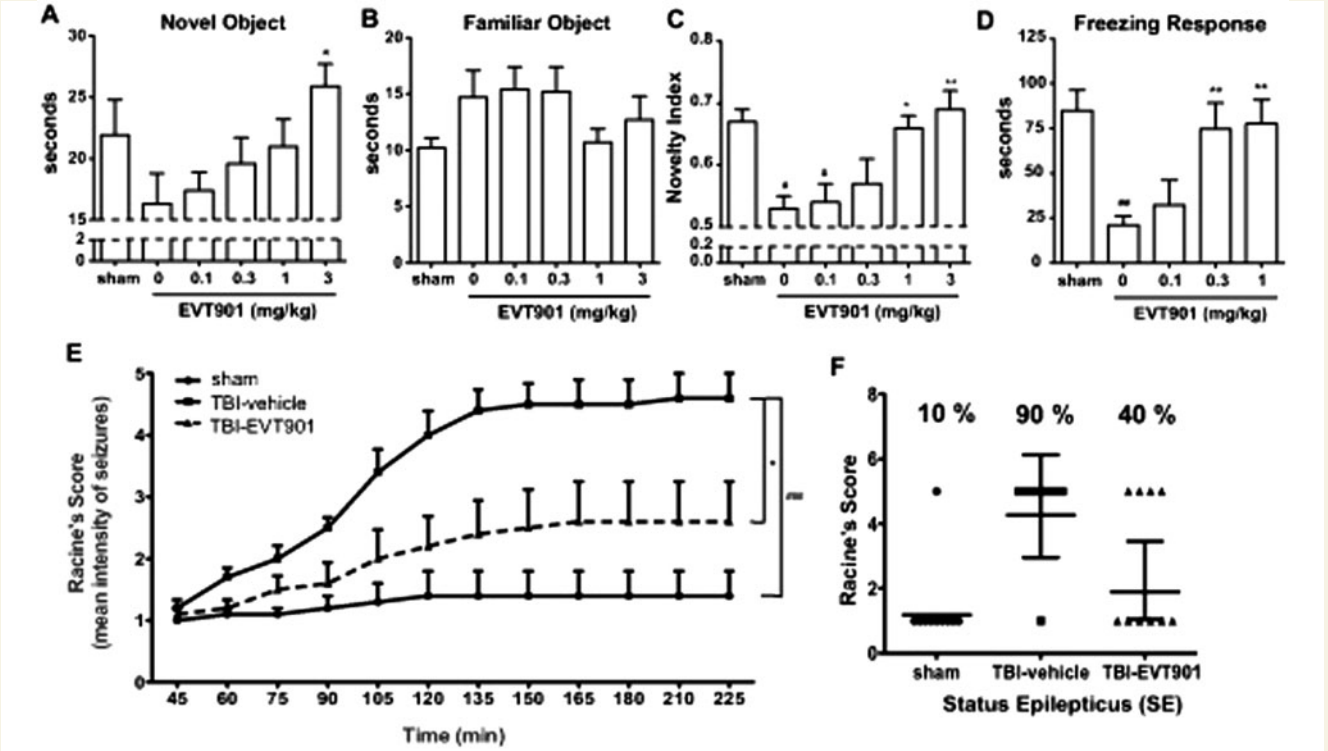

Figure 8 EVT901 improves functional recovery at 23 days after FPI-TBI and reduces post-TBI seizure activity. (**A–C**) Improvement in cognitive function after FPI-TBI evaluated by the object recognition test. Rats with a FPI-TBI or sham surgery were treated orally with vehicle alone or different doses of EVT901 (0.1, 0.3, 1 and 3 mg/kg) at 24 h post-surgery and once daily for 23 days. Recognition memory was evaluated using the Novel Object Recognition Test. (**A**) Time spent exploring novel (N) objects was recorded and expressed in seconds. There is a significant EVT901 effect on the novel object recognition test [two-way ANOVA with repeated measurement, $F(4,52) = 2.87$, $P < 0.05$]. $^{*}P < 0.05$ compared to 0 mg/kg. (**B**) There is no effects on familiar object recognition test [$F(4,52) = 1.10$, $P = 0.37$]. (**C**) The novelty index (N – F/N + F) was significantly reduced by TBI [$F(1,52) = 12.73$, $P < 0.001$]. EVT901 treatment improved recognition memory function as measured by the novelty index [$F(4,52) = 6.59$, $P < 0.0001$] $^{\#}P < 0.05$ compared to sham; $^{*}P < 0.05$ and $^{**}P < 0.005$ compared to 0 mg/kg; n = 9–10/group. (**D**) Improvement in recovery after TBI evaluated by the conditioned freezing response. TBI significantly reduced freezing responses [$F(1,55) = 13.84$; $P < 0.001$], while treatment with EVT901 preserved the freezing response [$F(3,55) = 5.68$: $P < 0.01$]; $^{\#\#}P < 0.005$ compared to sham; $^{**}P < 0.005$ compared to 0 mg/kg; n = 12/group. (**E**) Inhibition of kainate-induced seizure hypersensitivity after TBI by EVT901 (1 mg/kg). Evaluation of the increased susceptibility of rats to seizure induction by kainate was determined after a single injection of a sub-convulsant dose of kainate (8 mg/kg, intraperitoneally) in the different groups at 6 weeks after FPI-TBI. Seizure intensity was measured by Racine's score from 45 min to 3 h 45 min post-kainate injection. n = 10/group. There were significant time, EVT901, and time × EVT901 effects [two-way ANOVA with repeated measurement, time effect; $F(11,297) = 24.90$ $P < 0.0001$, EVT901 effect; $F(2,27) = 11.78$, $P < 0.0001$, time × EVT901 effect; $F(22,297) = 6.16$, $P < 0.0001$]. $^{\#\#\#}P < 0.0001$ compared to sham, $^{*}P < 0.05$ compared to TBI. (**F**) For each group, we defined a status epilepticus (SE) corresponding to the per cent of rats that reached continuous seizure activity in the different groups. Note that kainate treatment induced high numbers of seizure incidence (90%) in TBI-vehicle group, while EVT901 treatment reduced it to 40%. Results are given as mean ± SEM.

Discussion

The present results provide evidence that interfering with the oligomerization of p75NTR using the novel compound, EVT901 that interacts with the CRD of the extracellular domain of the molecule, is neuroprotective. P75NTR is structurally and functionally related to the TNFR superfamily. Although oligomerization is considered as the first signalling event induced by TNFRs, several studies indicate the presence of a pre-ligand binding assembly domain (PLAD) within the first cysteine-rich domain (CRD1) of the TNFR extracellular domain that mediates the pre-assembled oligomerization of the receptors prior to ligand stimulation (Chan, 2007). Such a PLAD domain has not been identified in p75NTR. Further, part of the pre-ligand binding oligomerization also has been attributed to cysteine bond formation in the transmembrane domain of p75NTR (Vilar *et al.*, 2009, 2014). However, reports show that mutations in CRD1 abrogate neurotrophin binding to the receptor, consistent with the possibility of an assembly event mediated by CRD1 as prerequisite for ligand binding (Baldwin and Shooter, 1995). In addition, a PLAD peptide from TNFR1 blocks TNF or collagen-induced arthritis *in vivo*, highlighting the PLAD region as an interesting pharmacological target for TNFRs (Deng *et al.*, 2005).

In this context, we developed a novel screening assay based on specific receptor binding that focused on the ligand-independent oligomerization of the p75NTR. Our

unpublished data indicated that consistent with previous findings (Vilar *et al.*, 2009), the CRD1 domain is important for oligomerization for inducing apoptosis with a mutant lacking CRD1 domain (data not shown). Therefore, our study first identified a potent small molecule, EVT901, which directly inhibits the pre-oligomerization of the p75NTR through its extracellular domain (CRD1 domain) at sub-nanomolar concentration.

Interestingly, a very recent study suggests that p75NTR coexists as a trimer along with a monomeric form at the cell surface (Anastasia *et al.*, 2015). However, trimerization was found not to be required for signalling (Anastasia *et al.*, 2015). The authors suggest that monomers of p75NTR are sufficient to induce apoptotic cell death and that oligomerization of p75NTR prevents cell death (Wang *et al.*, 2000; Anastasia *et al.*, 2015). Although we have not tested whether EVT901 affects trimerization of p75NTR, the inhibition of p75NTR oligomerization by EVT901 was supported by additional studies showing an inhibition of what we interpreted as oligomerization in a ligand-independent manner, after overexpression of tagged-p75NTR. This result suggests, for the first time, the presence of a specific self-association domain in the extracellular region of p75NTR, but does not rule out the possibility of trimerization. EVT901 also alters the ability of NGF to bind p75NTR (Fig. 1). Moreover, EVT901 is unable to bind to other TNFRs, confirming its specificity for p75NTR (Fig. 1). Interestingly, CRD1-p75NTR, the shorter form of p75NTR induced strong apoptosis and this is totally abrogated by EVT901 (Fig. 1).

The short p75NTR variant (s-p75NTR) has also been described and the complete absence of both p75NTR isoforms displays more severe phenotypes, but also leads to a persistent increase in the number of cholinergic neurons in the medial septum (von Schack *et al.*, 2001; Naumann *et al.*, 2002; Roux and Barker, 2002). Given the significance of cholinergic forebrain neurons in learning and memory processes and their degeneration in Alzheimer's disease, targeting p75NTR seems to be essential with regard to the modulation of the neuronal survival. S-p75NTR has been also reported to bind to Rabies virus glycoprotein through CRD1, and failed to bind neurotrophins (Langevin *et al.*, 2002).

Although p75NTR binds all neurotrophins with similar nanomolar affinities, this receptor also interacts with pro-neurotrophins (pro-NGF) and non-neurotrophin ligands including the neurotoxic aggregated prion protein fragment $PrP_{106–126}$ and amyloid-β peptide. Increased expression of these ligands promotes apoptosis in cultured neuronal cells and animal models of neurodegenerative diseases through activation of a p75NTR-dependent mechanism (Hempstead, 2002). Our studies show that pro-NGF, $PrP_{106–126}$ or amyloid-β ligands trigger cell death in neuroblastoma cells and these pro-apoptotic effects are strongly reduced by EVT901. Moreover, $PrP_{106–126}$ and amyloid-$\beta_{1–40}$ induce strong apoptosis in HEK cells transfected with full-length p75NTR or CRD1-p75NTR and are ineffective on the CRD1-deleted form of the receptor. While the precise binding site of both neurotoxic peptides on p75NTR has not been determined, our results suggest that their functional epitopes may be different from that of these neurotrophins and are probably located at the level of CRD1. Moreover, EVT901 could represent an innovative therapeutic approach for the treatment of many neurodegenerative diseases where neurotoxic p75NTR ligands are involved.

Many neuronal cells co-express Trk receptors and p75NTR that could form a high affinity binding complex with specificity in neurotrophin binding, and thus enhance Trk signalling and subsequent neurotrophic effects (Roux and Barker, 2002; Gentry *et al.*, 2004; Underwood and Coulson, 2008). EVT901 prevents ligand-independent apoptosis on cells overexpressing p75NTR, but also ligand-induced apoptosis in neuroblastoma cells expressing both p75NTR and Trk receptors, mainly by interfering directly with p75NTR oligomerization. Moreover, EVT901 stimulates neurite outgrowth, perhaps by enhancing the interaction between p75NTR and TrkA receptors, as supported by enhanced TrkA phosphorylation. Therefore, shifting the balance between p75NTR homo- to hetero-oligomerization can positively modulate the TrkA signalling pathway. Such modulation might be observed for other Trk receptor signalling pathways, such as TrkB, thereby increasing BDNF response, which could be beneficial in a wide range of contexts, particularly Huntington's disease. The ability of EVT901 to inhibit p75NTR death signalling and to enhance Trk, leading to both neuroprotective and neurotrophic signalling *in vitro*, suggests that this compound may be a disease-modifying drug candidate for the treatment of neurodegenerative disorders and/or CNS injury. Indeed, the beneficial effects of long-term treatment after TBI shown in our FPI-TBI study could reflect enhanced neural plasticity related to these neurotrophic effects. In addition, a recent study showed that proBDNF, which interacts with p75NTR, suppresses neuronal remodelling and synaptic plasticity in cleavage-resistant proBDNF knock-in mice (Yang *et al.*, 2014). Although we have not examined the potential involvement of proBDNF in our TBI studies, we can speculate that EVT901, through blocking p75NTR oligomerization, reduces proBDNF-induced p75NTR signalling in pathology after TBI.P75NTR has been shown to be upregulated in spinal cord injury, and to mediate apoptosis of oligodendrocytes via proNGF (Beattie *et al.*, 2002). Injury-induced apoptosis of oligodendrocytes appears to be related to cellular stress and inflammation (Sun *et al.*, 2010). Oligodendrocytes are also vulnerable to cell death in TBI and exhibit caspase-3 activation (Lotocki *et al.*, 2011). Here, we expanded that recent finding by showing that a CCI-TBI-induced rapid and transient expression of p75NTR, proNGF, and caspase-3, and that p75NTR was expressed in CC1-positive oligodendrocytes in the subcortical white matter. Thus, EVT901 given during the week after CCI-TBI preserved tissue integrity in the cortex and

corpus callosum, spared CC1-positive oligodendrocytes in the white matter and NeuN-positive cells in the cerebral cortex, and positively impacted neurological function.

Using a different TBI model, we gave tests of memory function to rats with FPI-TBI at 1 week following cessation of a 23-day EVT901 or vehicle oral delivery regimen. FPI-TBI produced severe memory deficits, indicated by the inability to recognize novel objects and by a severe reduction in freezing responses in the conditioned freezing paradigm. Daily oral administration of EVT901, beginning 24 h post-injury, significantly prevented the TBI-induced memory deficit with full recovery at 1 mg/kg/day. Interestingly, a 1-week treatment with EVT901 is sufficient to induce significant memory recovery (data not shown).

Moreover, significant cell death was observed in the hippocampus from 1–4 weeks after TBI and preceded emergence of kainite-induced hypersensitivity (Routbort *et al.*, 1999; Covolan and Mello, 2000; Dechant and Barde, 2002). In addition to its effects on cell death, and neurological and cognitive outcomes, EVT901 also significantly reduced TBI-induced hypersensitivity to pro-convulsive agents (Fig. 8E). EVT901 treatment also considerably reduced the per cent of rats exhibiting status epilepticus (prolonged seizures induced by pro-convulsive agents), a condition that induces marked alterations in neurotrophin expression and persistent apoptosis in hippocampal, piriform, and entorhinal cortical neurons, mediated to a large extent by activation of p75NTR signalling. Regarding the effect of EVT901, we hypothesize that blocking oligomerization of the p75NTR could prevent activation of the receptor alone or through its interaction with pro-neurotrophins, and might be related to the neuroprotective effects observed with EVT901 during the first week following trauma. Such effects may also prevent the decrease of mossy fibres and thus the abnormal sprouting process responsible for epileptogenesis.

The results of these two *in vivo* experiments suggest that proNGF-induced cell death, mediated by p75NTR, occurs in both neurons and oligodendrocytes after injury, and may contribute to both sensorimotor and cognitive dysfunctions after TBI. Post-injury microglial activation may lead to astrogliosis, and both activated microglia and astrocytes could be sources of proNGF leading to neuronal death through p75NTR signalling (Domeniconi *et al.*, 2007). P75NTR could also mediate apoptotic neuronal cell death during axonal degeneration (Harrington *et al.*, 2004). White matter injury, which leads to myelin debris fragments binding to Nogo receptor, may involve p75NTR signalling that contributes to axonal retraction and inhibition of endogenous repair mechanisms (Hempstead, 2006; Deinhardt *et al.*, 2011). Indeed, recent reports have shown that a different small molecule (LMA11-31A) that reportedly affects p75NTR signalling by different mechanisms can reduce cell death and enhance neurological function following spinal cord injury (Tep *et al.*, 2013), and can reduce the deleterious effects of TBI on adult neurogenesis (Shi *et al.*, 2013). Unlike LMA11-31A, which inhibits the binding of proNGF to p75NTR (Shi *et al.*, 2013; Tep *et al.*, 2013), EVT901 blocks the interaction of p75NTR through the CRD1 domain, resulting in prevention not only proNGF, but also proNTs and oligomers (such as amyloid peptide and prion peptide), that directly interact with p75NTR. Due to these specific mechanisms of EVT901, p75NTR could still interact with other co-receptor (such as Trks) to promote neuroregenerative effects including neurite outgrowth and neurogenesis.

Thus, EVT901, through direct interaction with p75NTR, could modulate multiple intracellular signalling mechanisms, including reducing the initial neuronal damage and subsequent axonal degeneration, and increase memory recovery. By activating neuronal repair, EVT901 may limit the secondary injury due to progression of the lesion, enhancing cognition and reducing the risk of hypersensitivity to pro-convulsive agents. Future studies are needed to further elucidate whether inhibitors of p75NTR oligomerization can promote neurogenesis and restore brain function after TBI. Recent reports from other laboratories certainly seem to support this approach (Shi *et al.*, 2013; Sebastiani *et al.*, 2015).

In summary, this study is the first report of a small molecule inhibitor of p75NTR pre-oligomerization, which directly interacts with the CRD1 domain of this receptor, strongly suggesting the presence of a PLAD domain. In addition, these results highlight the potential benefit of targeting the PLAD as a novel therapeutic approach to prevent activation of TNF receptor superfamily members. The novel mechanism of action of EVT901, its potency and selectivity, its ability to simultaneously block p75NTR death signalling and promote neuroprotective and neurotrophic effects make this a potentially useful compound for the treatment of TBI and other neurodegenerative diseases.

Acknowledgement

We would like to thank Xiaokui Ma for technical support in tissue sectioning.

Funding

This work was supported by NIH NS038079, with statistical support from NIH NS067092, UCSF/BASIC pilot funds, and a sponsored research agreement (SRA) between Sanofi R and D and UCSF.

Conflict of interest

EVT901 (formerly SAR127963) was developed by authors affiliated with Sanofi R and D. The license has now been transferred to Evotec, Inc, of which S.D-G. and F.B. are now employees. M.S.B. and S.L. received partial salary

support from the SRA between Sanofi R and D and UCSF. The other authors declare no competing financial interests.

Supplementary material

Supplementary material is available at *Brain* online.

References

Anastasia A, Barker PA, Chao MV, Hempstead BL. Detection of p75NTR trimers: implications for receptor stoichiometry and activation. J Neurosci 2015; 35: 11911–20.

Baldwin AN, Shooter EM. Zone mapping of the binding domain of the rat low affinity nerve growth factor receptor by the introduction of novel N-glycosylation sites. J Biol Chem 1995; 270: 4594–602.

Beattie MS, Harrington AW, Lee R, Kim JY, Boyce SL, Longo FM, et al. ProNGF induces p75-mediated death of oligodendrocytes following spinal cord injury. Neuron 2002; 36: 375–86.

Bunone G, Mariotti A, Compagni A, Morandi E, Della Valle G. Induction of apoptosis by p75 neurotrophin receptor in human neuroblastoma cells. Oncogene 1997; 14: 1463–70.

Chan FK. Three is better than one: pre-ligand receptor assembly in the regulation of TNF receptor signaling. Cytokine 2007; 37: 101–7.

Chan FK, Chun HJ, Zheng L, Siegel RM, Bui KL, Lenardo MJ. A domain in TNF receptors that mediates ligand-independent receptor assembly and signaling. Science 2000; 288: 2351–4.

Covolan L, Mello LE. Temporal profile of neuronal injury following pilocarpine or kainic acid-induced status epilepticus. Epilepsy Res 2000; 39: 133–52.

Dechant G, Barde YA. The neurotrophin receptor p75(NTR): novel functions and implications for diseases of the nervous system. Nat Neurosci 2002; 5: 1131–6.

Deinhardt K, Kim T, Spellman DS, Mains RE, Eipper BA, Neubert TA, et al. Neuronal growth cone retraction relies on proneurotrophin receptor signaling through Rac. Sci Signal 2011; 4: ra82.

Della-Bianca V, Rossi F, Armato U, Dal-Pra I, Costantini C, Perini G, et al. Neurotrophin p75 receptor is involved in neuronal damage by prion peptide-(106-126). J Biol Chem 2001; 276: 38929–33.

Deng GM, Zheng L, Chan FK, Lenardo M. Amelioration of inflammatory arthritis by targeting the pre-ligand assembly domain of tumor necrosis factor receptors. Nat Med 2005; 11: 1066–72.

Diarra A, Geetha T, Potter P, Babu JR. Signaling of the neurotrophin receptor p75 in relation to Alzheimer's disease. Biochem Biophys Res Commun 2009; 390: 352–6.

Domeniconi M, Hempstead BL, Chao MV. Pro-NGF secreted by astrocytes promotes motor neuron cell death. Mol Cell Neurosci 2007; 34: 271–9.

Gentry JJ, Barker PA, Carter BD. The p75 neurotrophin receptor: multiple interactors and numerous functions. Prog Brain Res 2004; 146: 25–39.

Harrington AW, Leiner B, Blechschmitt C, Arevalo JC, Lee R, Morl K, et al. Secreted proNGF is a pathophysiological death-inducing ligand after adult CNS injury. Proc Natl Acad Sci USA 2004; 101: 6226–30.

Hempstead BL. The many faces of p75NTR. Curr Opin Neurobiol 2002; 12: 260–7.

Hempstead BL. Dissecting the diverse actions of pro- and mature neurotrophins. Curr Alzheimer Res 2006; 3: 19–24.

Inoue T, Lin A, Ma X, McKenna SL, Creasey GH, Manley GT, et al. Combined SCI and TBI: Recovery of forelimb function after unilateral cervical spinal cord injury (SCI) is retarded by contralateral traumatic brain injury (TBI), and ipsilateral TBI balances the effects of SCI on paw placement. Exp Neurol 2013; 248C: 136–47.

Langevin C, Jaaro H, Bressanelli S, Fainzilber M, Tuffereau C. Rabies virus glycoprotein (RVG) is a trimeric ligand for the N-terminal cysteine-rich domain of the mammalian p75 neurotrophin receptor. J Biol Chem 2002; 277: 37655–62.

Lotocki G, de Rivero Vaccari JP, Alonso O, Molano JS, Nixon R, Safavi P, et al. Oligodendrocyte vulnerability following traumatic brain injury in rats. Neurosci Lett 2011; 499: 143–8.

Miller BA, Crum JM, Tovar CA, Ferguson AR, Bresnahan JC, Beattie MS. Developmental stage of oligodendrocytes determines their response to activated microglia *in vitro*. J Neuroinflammation 2007; 4: 28.

Naumann T, Casademunt E, Hollerbach E, Hofmann J, Dechant G, Frotscher M, et al. Complete deletion of the neurotrophin receptor p75NTR leads to long-lasting increases in the number of basal forebrain cholinergic neurons. J Neurosci 2002; 22: 2409–18.

Nykjaer A, Willnow TE, Petersen CM. p75NTR–live or let die. Curr Opin Neurobiol 2005; 15: 49–57.

Popovich PG, Guan Z, Wei P, Huitinga I, van Rooijen N, Stokes BT. Depletion of hematogenous macrophages promotes partial hindlimb recovery and neuroanatomical repair after experimental spinal cord injury. Exp Neurol 1999; 158: 351–65.

Routbort MJ, Bausch SB, McNamara JO. Seizures, cell death, and mossy fiber sprouting in kainic acid-treated organotypic hippocampal cultures. Neuroscience 1999; 94: 755–65.

Roux PP, Barker PA. Neurotrophin signaling through the p75 neurotrophin receptor. Prog Neurobiol 2002; 67: 203–33.

Schor NF. The p75 neurotrophin receptor in human development and disease. Prog Neurobiol 2005; 77: 201–14.

Sebastiani A, Golz C, Werner C, Schafer MK, Engelhard K, Thal SC. Proneurotrophin binding to P75 neurotrophin receptor (P75ntr) is essential for brain lesion formation and functional impairment after experimental traumatic brain injury. J Neurotrauma 2015; 32: 1599–1607.

Shi J, Longo FM, Massa SM. A small molecule p75(NTR) ligand protects neurogenesis after traumatic brain injury. Stem Cells 2013; 31: 2561–74.

Shuman SL, Bresnahan JC, Beattie MS. Apoptosis of microglia and oligodendrocytes after spinal cord contusion in rats. J Neurosci Res 1997; 50: 798–808.

Sun F, Lin CL, McTigue D, Shan X, Tovar CA, Bresnahan JC, et al. Effects of axon degeneration on oligodendrocyte lineage cells: dorsal rhizotomy evokes a repair response while axon degeneration rostral to spinal contusion induces both repair and apoptosis. Glia 2010; 58: 1304–19.

Tep C, Lim TH, Ko PO, Getahun S, Ryu JC, Goettl VM, et al. Oral administration of a small molecule targeted to block proNGF binding to p75 promotes myelin sparing and functional recovery after spinal cord injury. J Neurosci 2013; 33: 397–410.

Turner BJ, Murray SS, Piccenna LG, Lopes EC, Kilpatrick TJ, Cheema SS. Effect of p75 neurotrophin receptor antagonist on disease progression in transgenic amyotrophic lateral sclerosis mice. J Neurosci Res 2004; 78: 193–9.

Underwood CK, Coulson EJ. The p75 neurotrophin receptor. Int J Biochem Cell Biol 2008; 40: 1664–8.

Veiga S, Ly J, Chan PH, Bresnahan JC, Beattie MS. SOD1 overexpression improves features of the oligodendrocyte precursor response *in vitro*. Neurosci Lett 2011; 503: 10–4.

Vilar M, Charalampopoulos I, Kenchappa RS, Simi A, Karaca E, Reversi A, et al. Activation of the p75 neurotrophin receptor through conformational rearrangement of disulphide-linked receptor dimers. Neuron 2009; 62: 72–83.

Vilar M, Sung TC, Chen Z, Garcia-Carpio I, Fernandez EM, Xu J, et al. Heterodimerization of p45-p75 modulates p75 signaling: structural basis and mechanism of action. PLoS Biol 2014; 12: e1001918.

von Schack D, Casademunt E, Schweigreiter R, Meyer M, Bibel M, Dechant G. Complete ablation of the neurotrophin receptor

p75NTR causes defects both in the nervous and the vascular system. Nat Neurosci 2001; 4: 977–8.

Wang JJ, Rabizadeh S, Tasinato A, Sperandio S, Ye X, Green M, et al. Dimerization-dependent block of the proapoptotic effect of p75(NTR). J Neurosci Res 2000; 60: 587–93.

Weskamp G, Reichardt LF. Evidence that biological activity of NGF is mediated through a novel subclass of high affinity receptors. Neuron 1991; 6: 649–63.

Yaar M, Zhai S, Fine RE, Eisenhauer PB, Arble BL, Stewart KB, et al. Amyloid beta binds trimers as well as monomers of the 75-kDa neurotrophin receptor and activates receptor signaling. J Biol Chem 2002; 277: 7720–5.

Yang J, Harte-Hargrove LC, Siao CJ, Marinic T, Clarke R, Ma Q, et al. proBDNF negatively regulates neuronal remodeling, synaptic transmission, and synaptic plasticity in hippocampus. Cell Rep 2014; 7: 796–806.

Ye X, Mehlen P, Rabizadeh S, VanArsdale T, Zhang H, Shin H, et al. TRAF family proteins interact with the common neurotrophin receptor and modulate apoptosis induction. J Biol Chem 1999; 274: 30202–8.

Zhang H, Trivedi A, Lee JU, Lohela M, Lee SM, Fandel TM, et al. Matrix metalloproteinase-9 and stromal cell-derived factor-1 act synergistically to support migration of blood-borne monocytes into the injured spinal cord. J Neurosci 2011; 31: 15894–903.

Zhao YY, Shi XY, Qiu X, Zhang L, Lu W, Yang S, et al. Enriched environment increases the total number of CNPase positive cells in the corpus callosum of middle-aged rats. Acta Neurobiol Exp 2011; 71: 322–30.